Supporting Information

Red Aqueous Room-Temperature Phosphorescence Modulated by Anion-π and Intermolecular Electronic Coupling Interactions

Fengbo Liu,[a] Hai Yang,[a] Dongdong Sun,[a] Fang Gao,[a] Xiongzhi Zhang,[a,b] Zhiyong Zhao,[a,b] Xie Han,[a,b] and Simin Liu*[a,b]

[a] School of Chemistry and Chemical Engineering, Wuhan University of Science and Technology, Wuhan 430081, China. E-mail: liusimin@wust.edu.cn.
[b] The State Key Laboratory of Refractories and Metallurgy, Institute of Advanced Materials and Nanotechnology, Wuhan University of Science and Technology, Wuhan 430081, China.

DOI: 10.1039/x0xx00000x

Table of Contents

Experimental Procedures

Materials, instrumentation and measurements

All chemicals and solvents for synthesis were purchased commercially. 2Br-NDA[1, 2] and 2Br-NDI(P)[3, 4] were prepared according to reported methods. High-purity 2Br-NDI was synthesized by modified method in George's work[5] and purified by silica gel column chromatography in the presence of KPF_6. The counterion was exchanged to chloride anion by Amberlite® IRA-400(Cl) resin (from Sigma-Aldrich, washed thoroughly with ultra-pure water before use). Ultra-pure water was used for all analytical experiments and also single crystal cultivation. CB[*n*]s (*n* = 7, 8, 10) were prepared according to reported methods.[6, 7] Acid-free CB[7] used here was purified by silica gel column chromatography (water : acetic acid : formic acid = 10:10:1) followed by repeated evaporation of water from the aqueous suspension of CB[7] until the pH was ~7.[8]

NMR researches were performed on Agilent 600 MHz DD2 spectrometer equipped OneNMR probe. S2pul sequence was used for 1D **1H and 13C NMR** measurements. Scan number of 21500 was set for the ^{13}C NMR spectrum. The acquisition time was 0.918 s and the spectral width was 35714.3 Hz. **COSY, NOESY and ROESY** were recorded using gCOSY, NOESY and ROESY pulse sequences, respectively. The 2D spectra recorded were processed and analysed using MestReNova software.[9] For **COSY** spectrum, sine square 0.0˚ was set as window function along f2 and f1 before applying the baseline correction (Bernstein Polynomials Fit, with a polynomial order of 3 applied to all dimensions). COSY-like symmetrization and Reduce t1 Noise were used to get a cleaner spectrum. For **ROESY** spectra, sine square 90˚ and sine bell 90˚ were set as window function along f_2 and f_1, respectively, with first point of 0.5. Phases in both of the f_1 and f_2 dimension were manually corrected before applying the same baseline correction. The **Exchange Spectroscopy (EXSY)** experiment was conducted by recording two ROESY spectra upon water suppression, with mixing time of 0 ms (as reference) and 500 ms, respectively. Values of k_1 and k_{-1} were calculated using the EXSYCalc software developed by MestreLab.[10] Only positive contours were shown and used for volume integral. **DOSY** spectra were recorded using the Dbppste (DOSY bipolar pulse pair stimulated echo) sequence at 298 K. The hydrated diameter could be calculated by the Stokes-Einstein equation:

$$D = \frac{k_b T}{6\pi\eta r_h}$$

In which k_b is the Boltzmann's constant ($m^2 \cdot kg \cdot s^{-2} \cdot K^{-1}$), T is the temperature in Kelvin (298 *K*), η is the dynamic viscosity of deuterium water (0.9142551 x 10^{-3} $kg \cdot m^{-1} \cdot s^{-2}$ at 298 *K*), r_h is the hydrodynamic radius of the spherical particle.

ESI-MS spectra were recorded on a 9.4 T high-resolution FT-MS mass spectrameter (Solarix 9.4 T) from Bruker in the positive polarity.

UV-Vis titrations were performed on a SHIMADZU UV-VIS-NIR spectrophotometer (UV-3600) at room temperature with resolution of 0.1 nm. A 1 mm × 1 cm cell was used for operation. The scan range was from 200 to 700 nm using intermediate speed and a slit width of 2.0 nm. Samples for UV-Vis titrations were prepared by mixing various volumes of the aqueous solution of 50 μM 2Br-NDI and 50 μM 2Br-NDI complexed with 4.0 eq. CB[7] and 1.0 eq. CB[8] and 0.5 eq. CB[10], respectively.

Steady and gated emission spectra were recorded on a PerkinElmer LS-55 machine equipped with a Xenon discharge lamp, gated photomultiplier and Monk-Gillieson type monochromators. The spectra were recorded under single scan model at speed of 500 nm/min. Gated emission was recorded by phosphorescence mode with a delay time of τ_{delay}=0.06 ms and a gated time of τ_{gated}=0.04 ms. The measurements was conducted with 20 ms for each cycle with 1 flash count. Dark current was set at the beginning and kept for all continued measurements under the same parameters. Samples of 2Br-NDI with various concentrations (from 8.0 mM to 3.9 μM) in the presence of excess CB[7], 1.0 eq. CB[8] and 0.5 eq. CB[10] were prepared by diluting their stock solutions from [2Br-NDI]=8.0 mM. Emission in N_2 was performed by bubbling samples with high-purity N_2 for 10 min before immediate recording.

Steady and gated 3D emission-excitation spectra were recorded under the 3D scan model on the same machine. For better results, concentration of 2Br-NDI at 125 μM was used for 2Br-NDI in the absence and presence of CB[7] and CB[8], while the CB[10]·$(2Br\text{-}NDI)_2$ complex was recorded with [2Br-NDI]=500 μM. Excitation and emission slits were adjusted according the emission intensity of the pre-scanned emission-excitation spectra and finally set as shown in Table S1. Long-time protection in N_2 during recording was realized by firstly bubbling the aqueous solutions by N_2 for 10 min and then keeping the samples in N_2 environment by connecting a positive-pressure N_2 bag through silica gel tube. Steady emissions excited at 385 nm right before and immediately after completing scans were compared to ensure the hermeticity of N_2 environment during the whole recording process.

Table S1. Parameters setting for recording steady and gated 3D emission-excitation spectra of 2Br-NDI in the absence and presence of CB[*n*]s (*n* = 7, 8, 10) in N_2.

Components	$Slit_{Ex}$/$Slit_{Em}$ for steady Em-Ex	$Slit_{Ex}$/$Slit_{Em}$ for gated Em-Ex	τ_{delay} / τ_{gate} for gated Em-Ex
2Br-NDI	3 nm / 12 nm	3 nm / 12 nm	60 μs / 100μs
CB[7]$_2$·(2Br-NDI)	3 nm / 12 nm	3 nm / 12 nm	60 μs / 40μs
CB[8]·(2Br-NDI)	6 nm / 12 nm	3 nm / 12 nm	60 μs / 40μs
CB[10]·$(2Br\text{-}NDI)_2$	5 nm / 12 nm	3 nm / 12 nm	60 μs / 40μs

Dynamic light scattering (DLS) was recorded by the Particle Sizing Systems on a NICOMP 380 Z3000 analyser with a running time for 15 min until balanced Gaussian calculation history curves were given. Number-weighted NICOMP distribution analysis was used for results analyses. Samples for the DLS analysis were taken from the stock solutions for the measurements of steady and gated emission spectra.

Fluorescent/phosphorescent lifetime and quantum yields were measured on Edinburgh FLS980 steady-state transient fluorescence/phosphorescence spectrometer. Frequency at 40 Hz and photon count at 8000 for the measurement of phosphorescent lifetime. Measurements under N_2 protection was realized by bubbling samples with N_2 for 10 min before immediate recording. Fluorescent range in 400-520 nm and phosphorescent range in 600-800 nm were integrated for quantum yield calculation.

DFT and TDDFT: simulations for the optimized structure of 2Br-NDI, orbital energy levels and the analysis for electrostatic potential were carried out by all-electron DFT calculations, which was performed by the latest version of ORCA quantum chemistry software (Version 5.0.1).[11] The corrected version of B97 exchange-correlation functional proposed by Grimme (so-called B97-3c)[12] was adopted for all calculations. The B97-3c functional, which is based on the well-known B97 functional[13], is a highly efficient method which utilizes three corrections namely: the D3BJ method[14] including three-body term to account for long-range dispersion interactions, a short range bond-length correction (SRB) which corrects for systematically overestimated covalent bond-lengths for electronegative elements and a modified stripped-down triple-ζ basis (def2-mTZVP) to obtain accurate geometries and relative energies. The nature of noncovalent interaction was studied by using IGM (Independent Gradient Model) method through Multiwfn software.[15] The visualization of IGM and orbitals were rendered by VMD.[16] The binding energy between Cl^- and 2Br-NDI core in water was calculated by the following formula: $E_{binding}=E_{complex}-[E(2Br\text{-}NDI^{2+})+E(Cl^-)]$, where the $E_{complex}$= -7519.79482 hartree, $E(2Br\text{-}NDI^{2+})$= -7059.435225 hartree and $E(Cl^-)$= -460.3453872 hartree. TDDFT was performed using the B3LYP functional together with the def2SVP basis set, and the spin-orbit coupling (SOC) was analysed by the method of spin-orbit mean-field (SOMF). The singlet and triplet excited states energy levels and transition orbitals contribution for CB[8]·(2Br-NDI) and 2Br-NDI were given by loading the .out files in the Multiwfn software and analysed by the subfunction “15 Print major MO transitions in all excited states” in the function “18 electron excitation analysis”.[15]

Single crystal cultivation for the the 2Br-NDI was performed by slow evaporation of its aqueous solution at high concentration in a desiccator filled with $MgSO_4$ for about 1 month. Large-area and colorless slide crystal was easily given for X-ray diffraction measurement. The single crystal of CB[8]·(2Br-NDI) was provided by standing the aqueous solution of CB[8] • (2Br-NDI) (2 mL for each sample) in the presence of KI, with the concentrations of 2Br-NDI at 8.0, 4.0, 2.0, 1.0, 0.5, 0.25 and 0.125 mM. For each concentration, 600 mM aqueous solution of KI was added by small batches (20 μL) to find a critical volume (V_{CPC}, mL) of KI solution and then another four controlled groups with different volumes (75%, 50%, 25% and 12.5% V_{CPC}) of 600 mM KI solution were prepared with 2Br-NDI at the same concentration. All samples were sealed and heated at 80 °C for 5 min and then cooled to R.T. Red single crystals for analysis were obtained after standing in sealed flask at R.T over 1 month.

Single Crystal X-ray diffraction data for the 2Br-NDI were collected using a Bruker-AXS D8 Quest diffractometer (Mo Kα, λ= 0.71073 Å) at 298 K, while the CB[8]·(2Br-NDI) crystal were collected using a Bruker-AXS D8 Venture diffractometer (Ga Kα, λ= 1.34139 Å) at 100 K. Indexing was performed using APEX3 (Difference Vectors method). Data integration and reduction were performed using SaintPlus. Absorption correction was performed by multiscan method implemented in SADABS. Space groups were determined using XPREP implemented in APEX3. Structures were solved using SHELXL-2014 (direct methods) and refined using SHELXL-2014 (full-matrix least-squares on F^2) with anisotropic displacement contained in APEX3 program packages. Hydrogen atoms on carbon and nitrogen were calculated in ideal positions with isotropic placement parameters set to 1.2 × U_{eq} of the attached atoms.

Scanning electron microscope (SEM) was performed on a field emission scanning electron microscope (Nova NanoSEM400). The sample for SEM was preparing by neutral drying of the aqueous solution of 125 μM 2Br-NDI on a silica substrate.

Cyclic voltammograms was recorded on an electrochemical workstation (CHI 760E) using 0.5 mM 2Br-NDI in the absence and presence of 1.0 eq. CB[8]. The scan range was -1.4 - 0.2 V and the scan rate was 100 mV/s. A 10 mL single-compartment glass cell was fitted with a working glassy carbon electrode (3 mm), a Pt (0.5*37 mm) auxiliary electrode and an Ag/AgCl (6 mm) reference electrode. All solutions were degased with N_2 for 5 min and sealed before measurements.

Synthesis of 2Br-NDI (chloride salt)

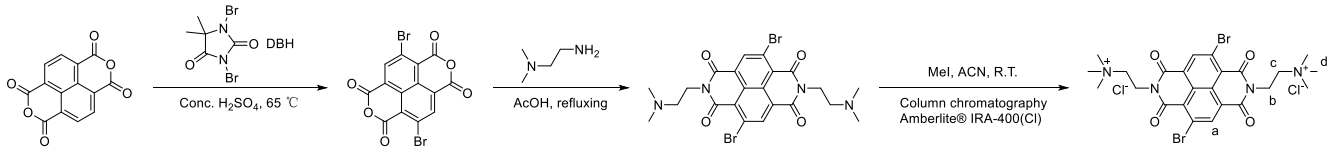

3.29 g (5.81 mmol) 2Br-NDI(P) was mixed and stirred with excess MeI in 10 mL ACN at R.T. over night. After the completion of reaction (TLC monitoring: DCM:ACN=2:1 in the presence of solid KPF_6), additional ACN and excess KPF_6 were added to completely dissolve the suspension (Note: incomplete counter anion exchange will influence the following column chromatography procedure and the final yield of product, small volume of water could be added to promote the dissolution process). The red filtrate after filtration was evaporated to dryness and the residue was washed with water to remove extra KPF_6 until the supernatant just turned from colorless to pale-red (Note: uncompleted removal of KPF_6 will inhibit the absorption process, induce fractions crossing and loss during column chromatography). The solid PF_6^- salt was redissolved in ACN, absorbed on 6 g 100-200 meshed silica gel and purified by flashed silica gel column chromatography under pressure (D = 6 cm, H = 16 cm), gradiently eluted with DCM:ACN=10:1→5:1→3:1→1:1 in the presence of excess KPF_6 (column equilibrium was performed using mixed solvent of

DCM:CAN=10:1). The yellow band on column were eluted, collected as light brown solution, evaporated to dryness and then washed with water to remove KPF_6. 3.6 g pure 2Br-NDI in chloride salt was given in yield of 93 % after thorough counter anion exchange in water using Amberlite® IRA-400(Cl) resin (by simply shaking the suspension of the PF_6^- salt and resin in water overnight) and lyophilization. ^{1}H NMR (600 MHz, D_2O, 298 K, Figure S1): δ = 9.06 (s, 2H), 4.72-4.65 (m, 4H), 3.74-3.69 (m, 4H), 3.36 (s, 18H). ^{13}C NMR (150 MHz, D_2O, 298 K, Figure S2), δ (ppm) = 161.88, 161.82, 138.72, 128.12, 127.54, 124.99, 124.12, 61.60, 53.30, 34.68. ESI-MS (Figure S3): m/z ($C_{24}H_{28}Br_2N_4O_4^{2+}$): 297.023544 (calc.: 297.023316, mean error=-0.4 ppm).

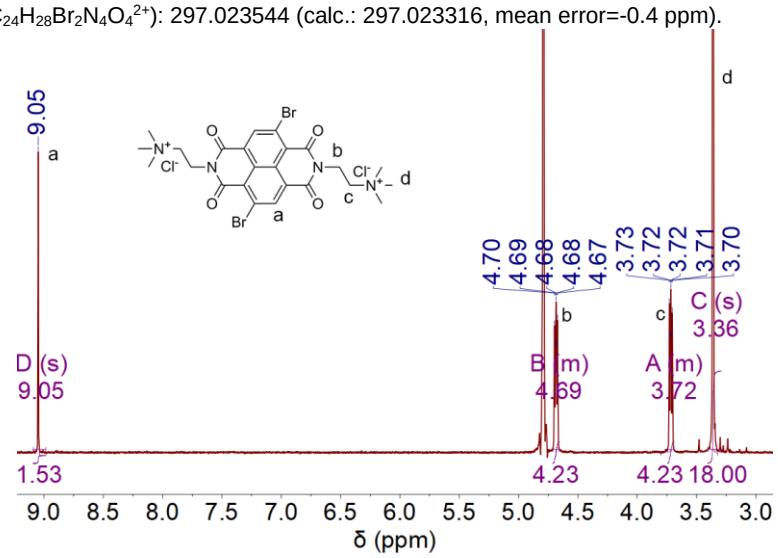

Figure S1. ^{1}H NMR (600 MHz, D_2O, 298 K) of 2.0 mM **2Br-NDI** (chloride salt).

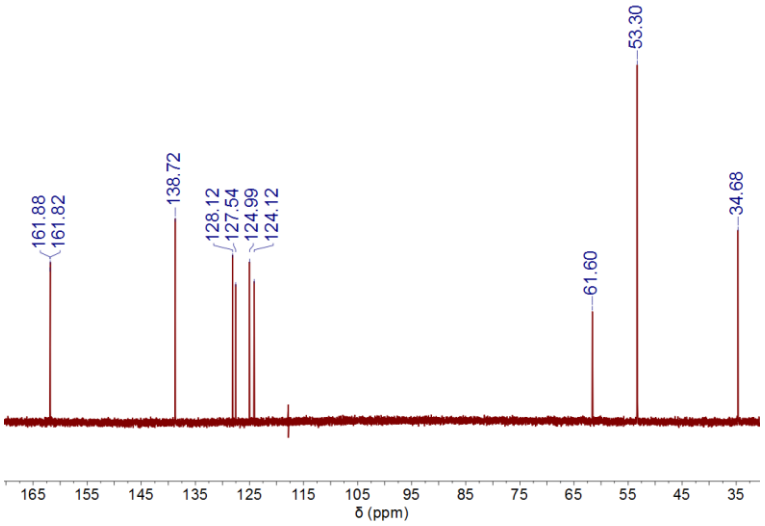

Figure S2. ^{13}C NMR (150 MHz, D_2O, 298 K) of 8.0 mM **2Br-NDI**.

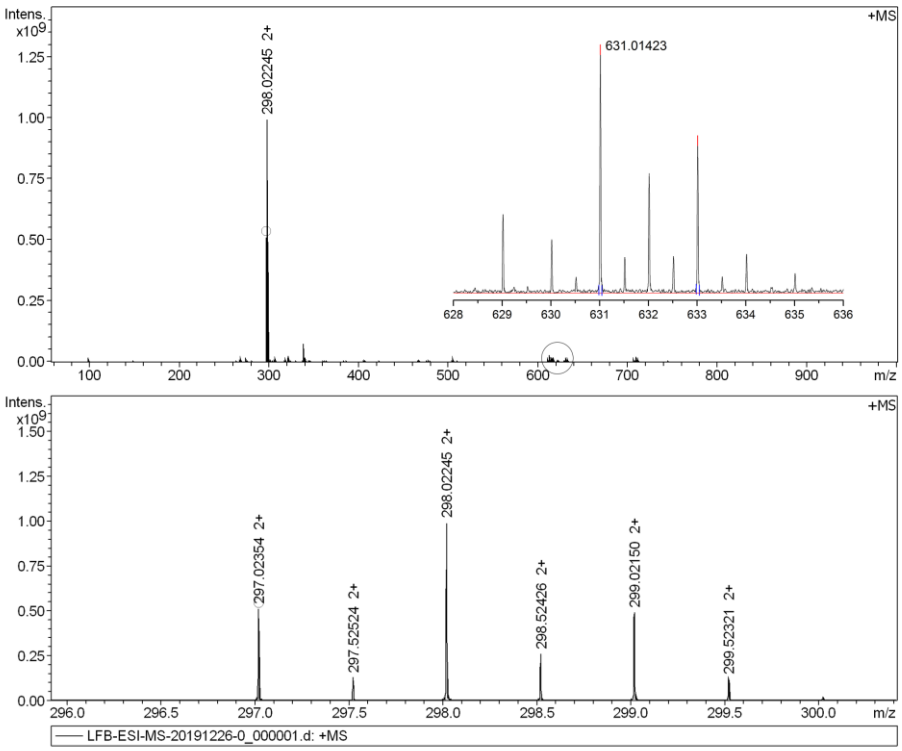

Figure S3. Full and partial ESI-MS spectra of **2Br-NDI** (positive polarity).

Experiment Results

Properties researches for 2Br-NDI

RTP lifetime of aqueous 2Br-NDI at various concentrations

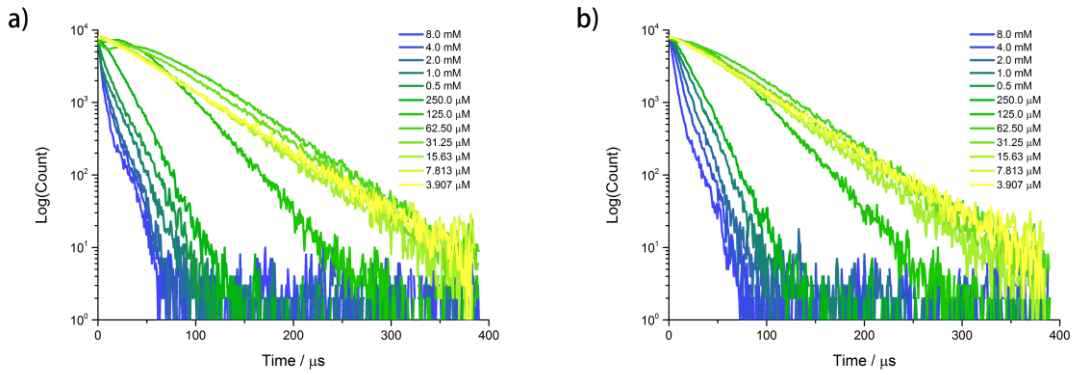

Figure S4. Concentration dependence of lifetime (λ_{Ex} = 385 nm) at a) 583 nm, b) 621.5 nm of 2Br-NDI in N_2.

Scanning electron microscope (SEM) and single crystal analysis

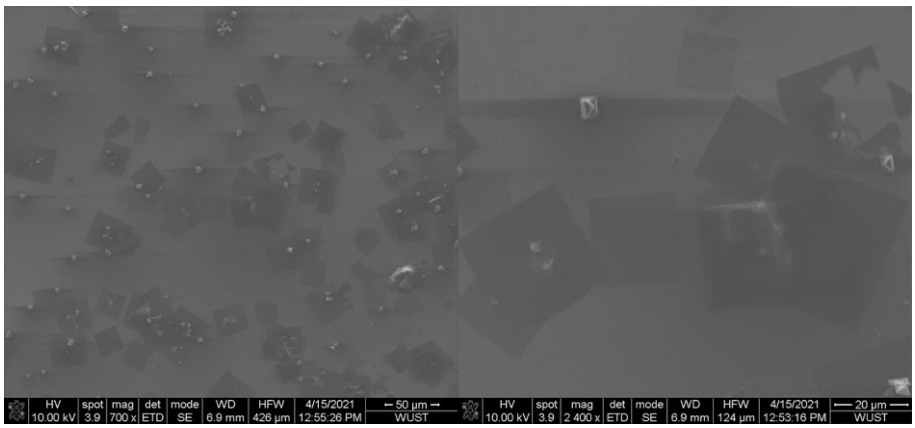

Figure S5. SEM for the 2Br-NDI.

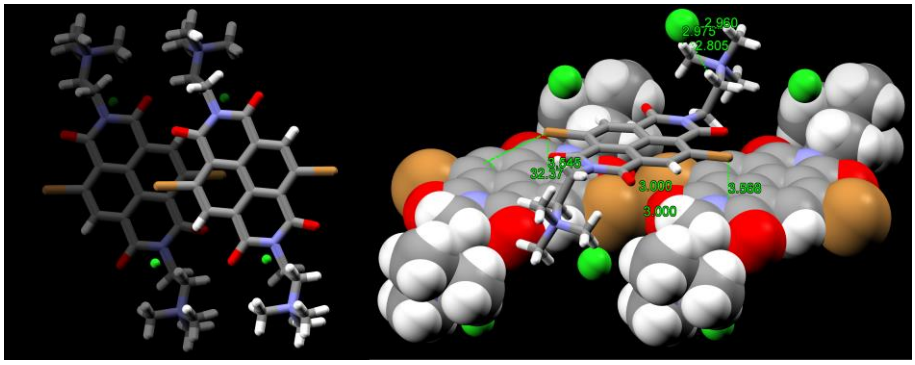

Figure S6. Single crystal structures of the 2Br-NDI.

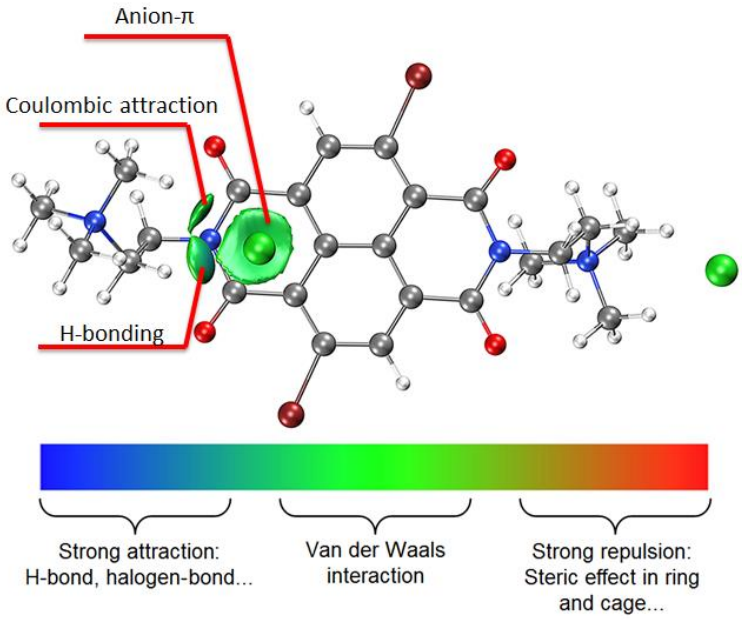

Figure S7. Synergistic interaction between Cl^- and 2Br-NDI core from DFT simulation by independent gradient model (IGM).(Blue color indicates H-bonding interactions, green color indicates the dispersive forces).

Diffusion Ordered Spectroscopy (DOSY)

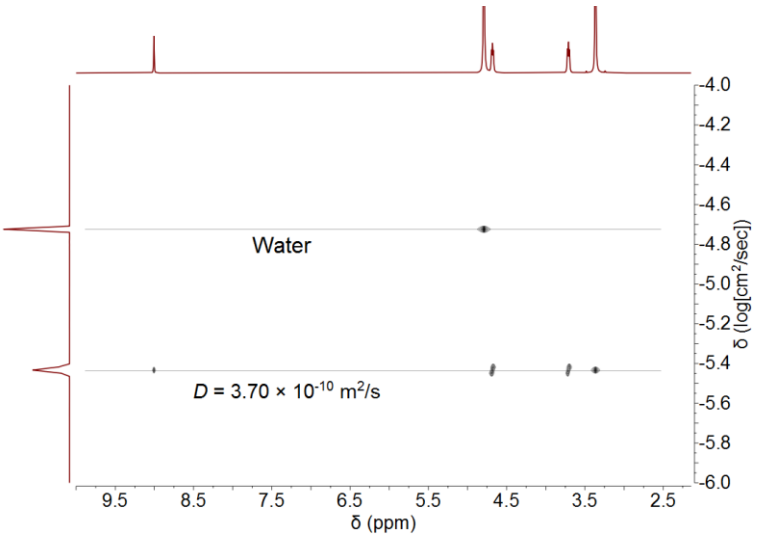

Figure S8. DOSY of 8.0 mM 2Br-NDI.

Further evidences for anion-π interaction and the anion-π induced long-lived emission of 2Br-NDI

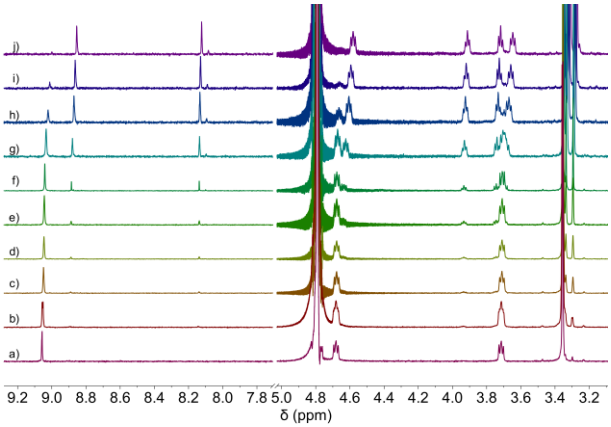

Figure S 9. ^{1}H NMR (600 MHz, D_2O, 298 K) of 1.0 mM 2Br-NDI in the presence of a) 0 eq. b) 10 eq., c) 25 eq., d) 50 eq., e) 75 eq., f) 125 eq., g) 250 eq., h) 500 eq., i) 750 eq., j) 1000 eq. of NaF(saturated).

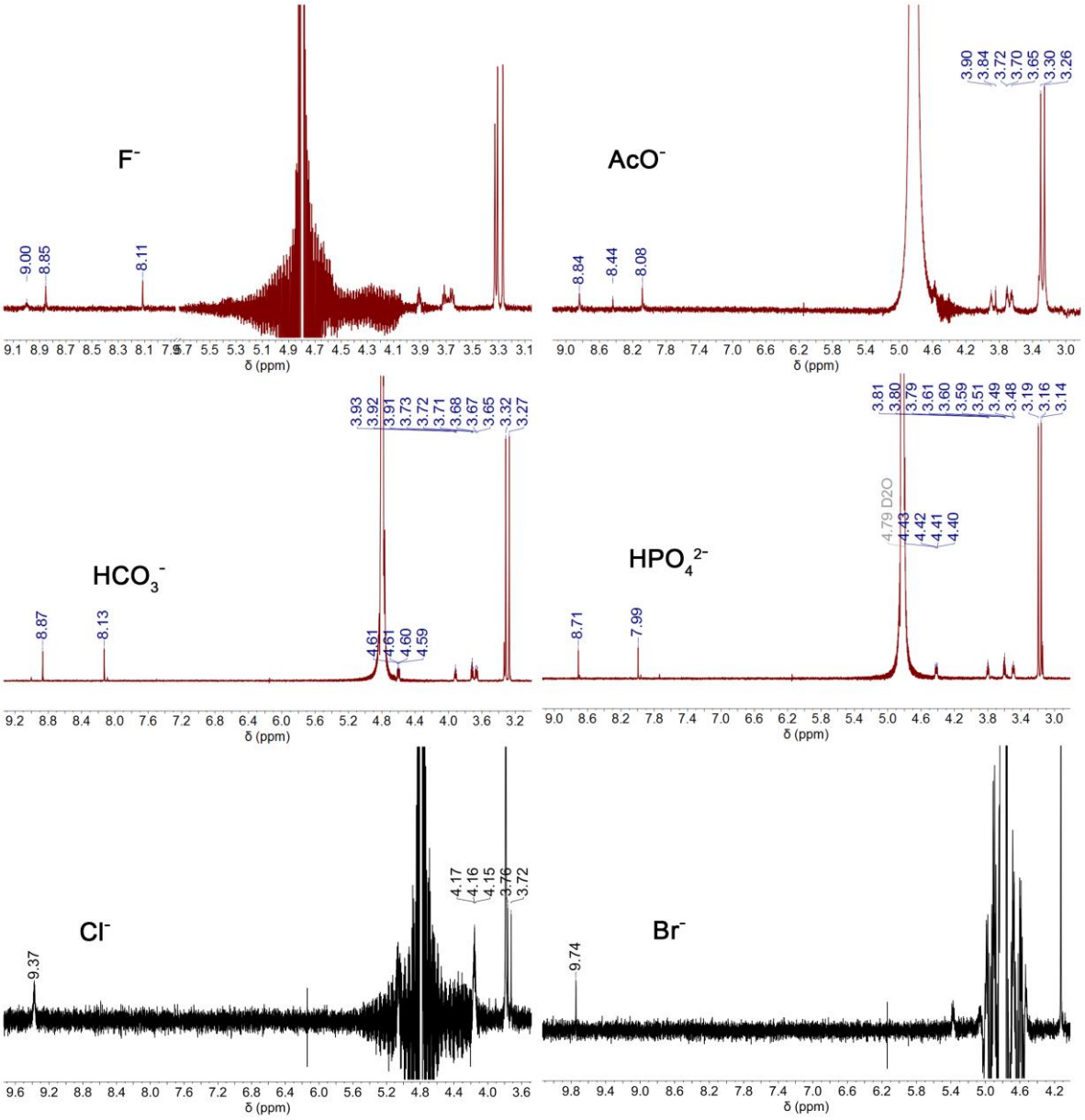

Figure S 10. ^{1}H NMR (600 MHz, D_2O, 298 K) of 1.0 mM 2Br-NDI upon addition of excess sodium salts of different anions (F^-, AcO^-, HCO_3^-, HPO_4^{2-}, Cl^-, and Br^-)

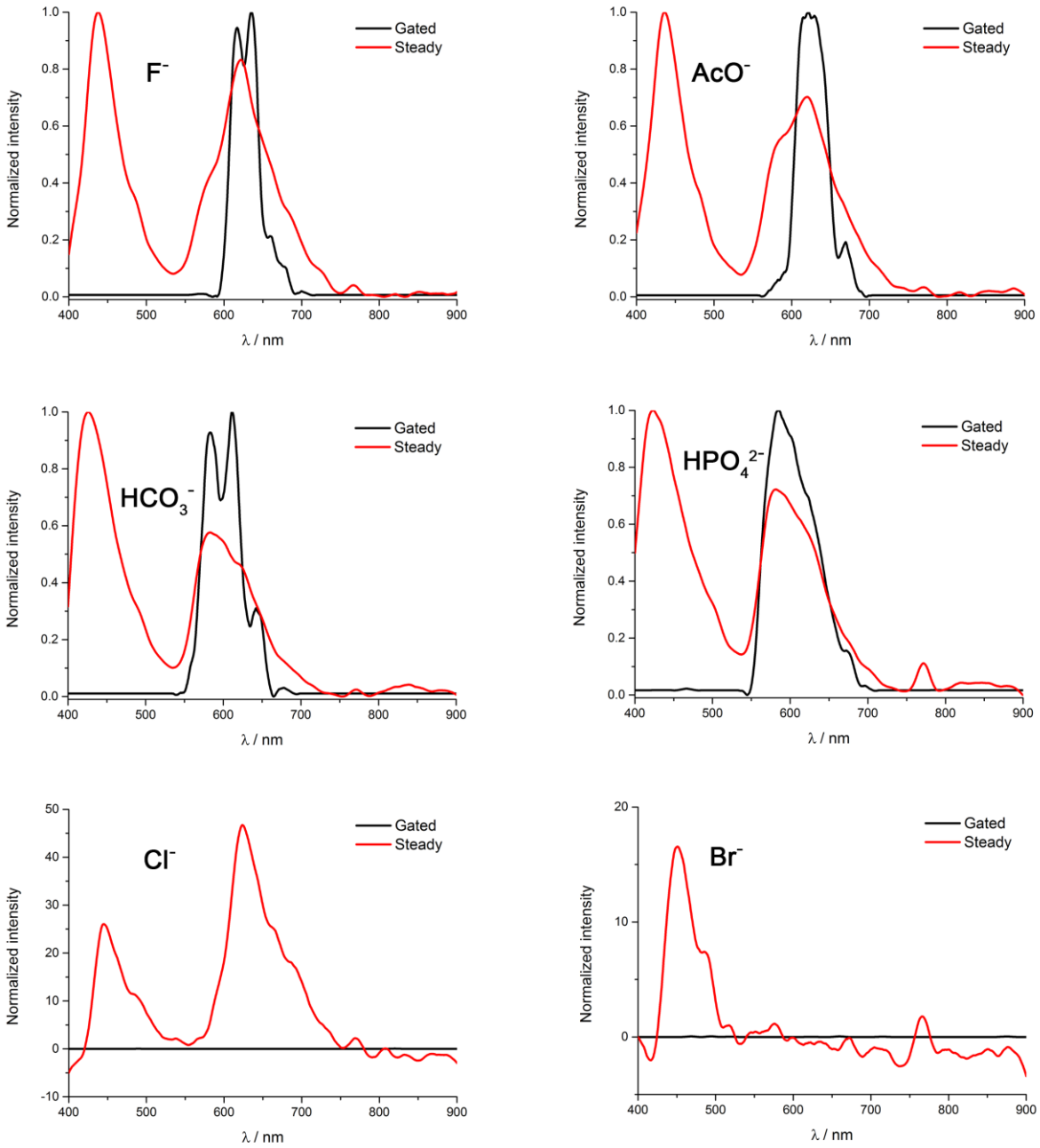

Figure S 11. Steady and gated emission of 0.5 mM 2Br-NDI in N_2 upon addition of 1000 eq. sodium salts of different anions (F^-, AcO^-, HCO_3^-, HPO_4^{2-}, Cl^-, and Br^-). (λ_{Ex} = 385 nm, $slit_{Ex}$ = 6 nm, $slit_{Em}$ = 10 nm, τ_{delay}=0.06 ms, τ_{gate}=0.04 ms)

Excitation spectra and CT-excited emission spectra

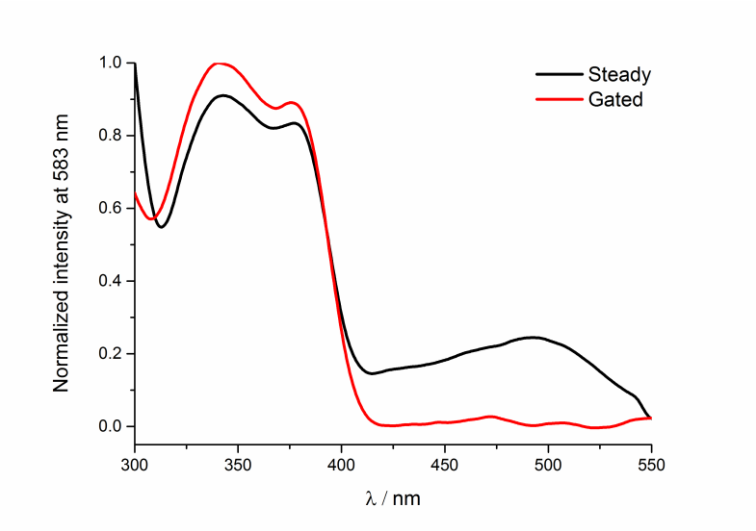

Figure S12. Steady and gated excitation spectra of 125 µM 2Br-NDI at 583 nm in N_2 ($slit_{Ex}$ = 4.0 nm, $slit_{Em}$ = 18.0 nm, τ_{delay}=0.04 ms, τ_{gate}=0.04 ms).

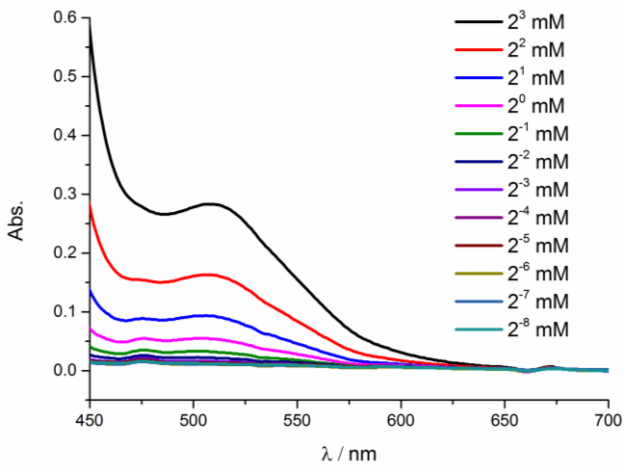

Figure S13. UV-Vis spectra of 2Br-NDI at various concentrations.

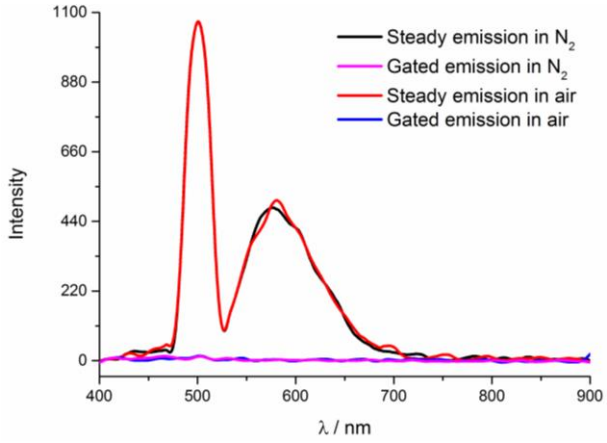

Figure S14. Steady and gated emission of 0.125 mM 2Br-NDI in N_2 and air upon CT excitation. (λ_{Ex} = 502 nm, $slit_{Ex}$ = 3.5 nm, $slit_{Em}$ = 12.5 nm, τ_{delay}=0.06 ms, τ_{gate}=0.04 ms).

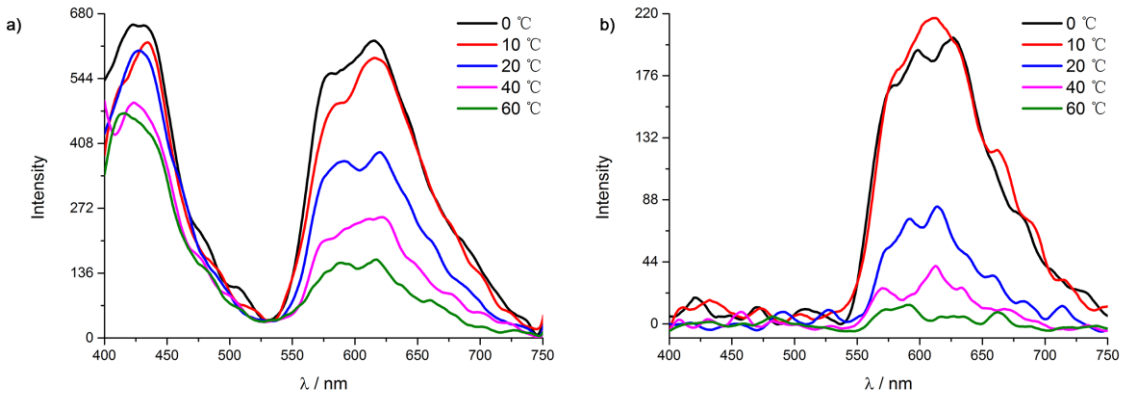

Figure S15. a) Steady and b) gated emission of 0.125 mM 2Br-NDI at various temperature in N_2 (λ_{Ex} = 385 nm, $slit_{Ex}$ = 3.5 nm, $slit_{Em}$ = 12.5 nm, τ_{delay}=0.06 ms, τ_{gate}=0.04 ms).

Host-guest recognition between CB[*n*]s (*n* = 7,8,10) and 2Br-NDI

CB[7]$_2$·(2Br-NDI)

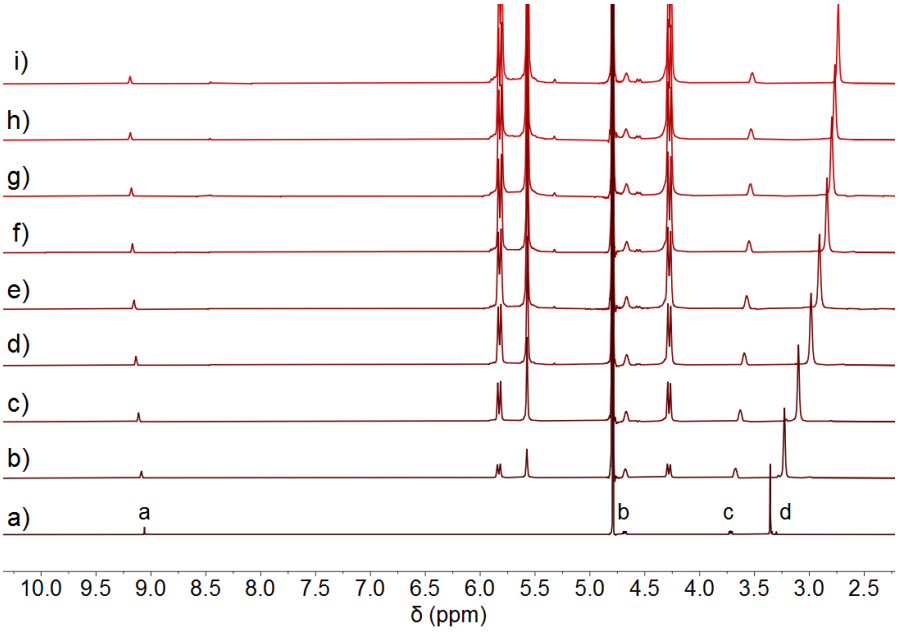

Figure S16. ^{1}H NMR titration of 1.0 mM 2Br-NDI in the presence of a) 0, b) 0.5, c) 1.0, d) 1.5, e) 2.0, f) 2.5, g) 3.0, h) 3.5, i) 4.0 eq. CB[7].

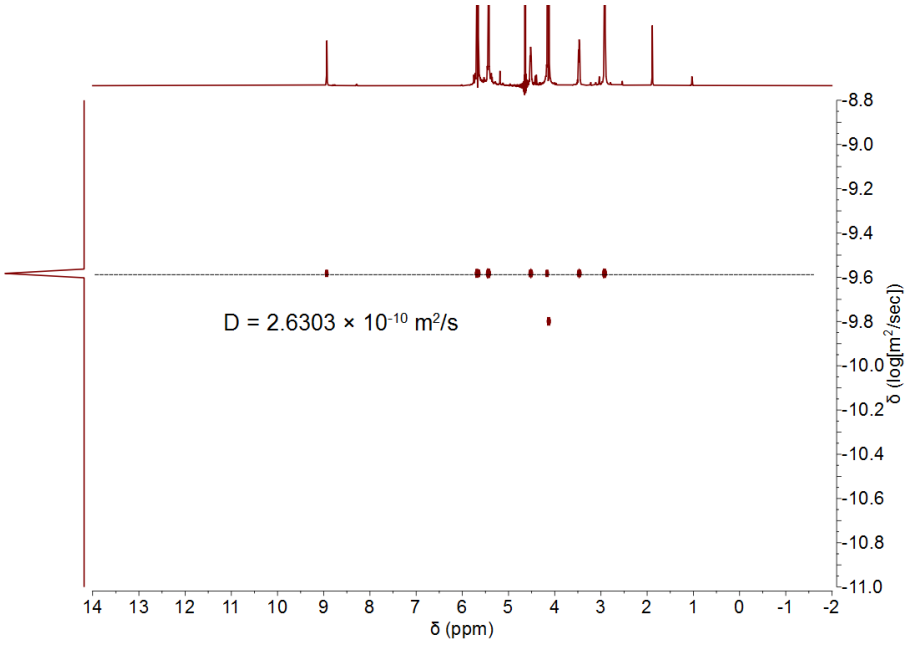

Figure S17. DOSY spectrum of 8.0 mM 2Br-NDI in the presence of excess CB[7] (hydrated diameter d_h = 1.8 nm).

CB[8]·(2Br-NDI)

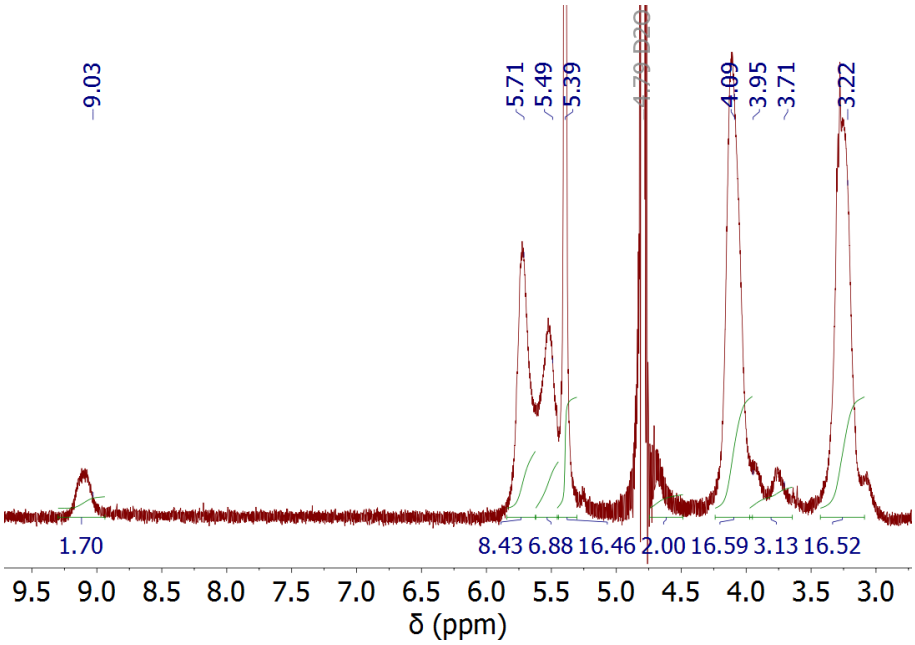

Figure S18. ^{1}H NMR integral of 1.0 mM 2Br-NDI in the presence of 1.1 eq. CB[8].

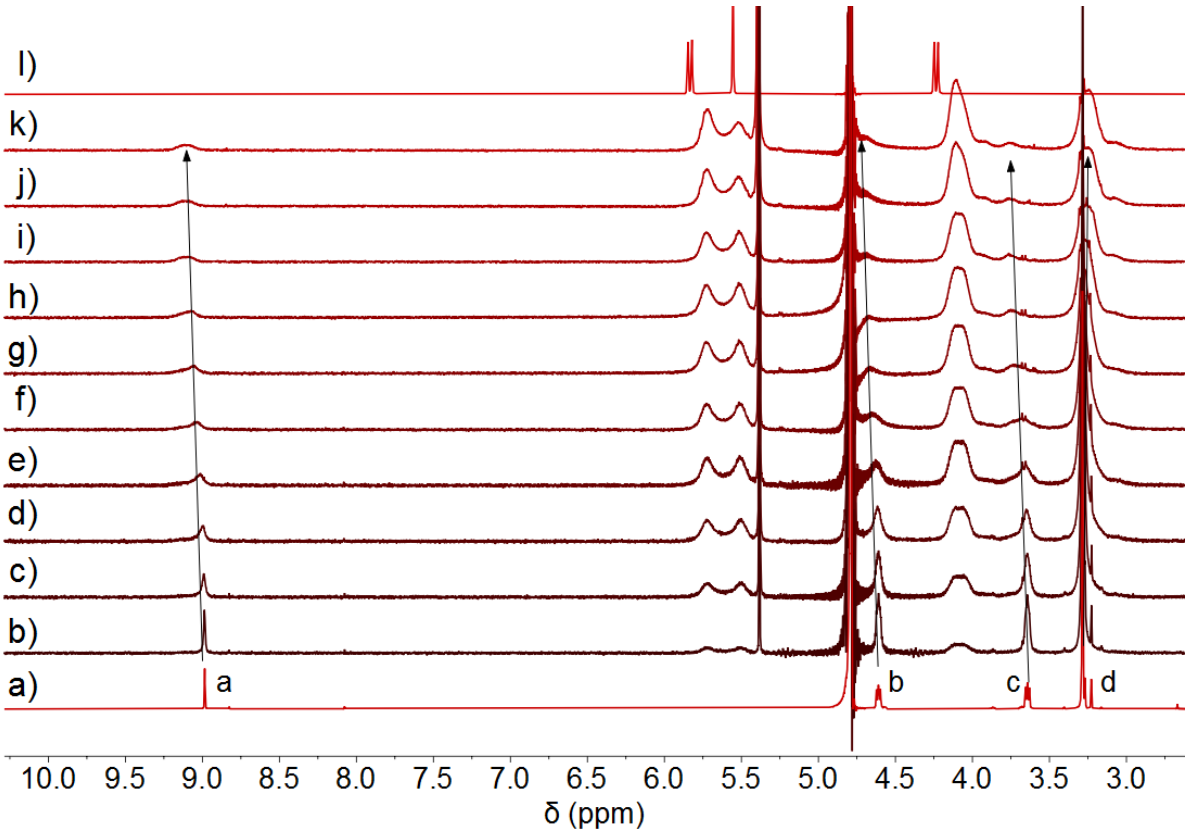

Figure S19. ^{1}H NMR titration of a) 1.0 mM 2Br-NDI b-k) upon equivalently adding CB[8] to 1.1 eq. and l) CB[8].

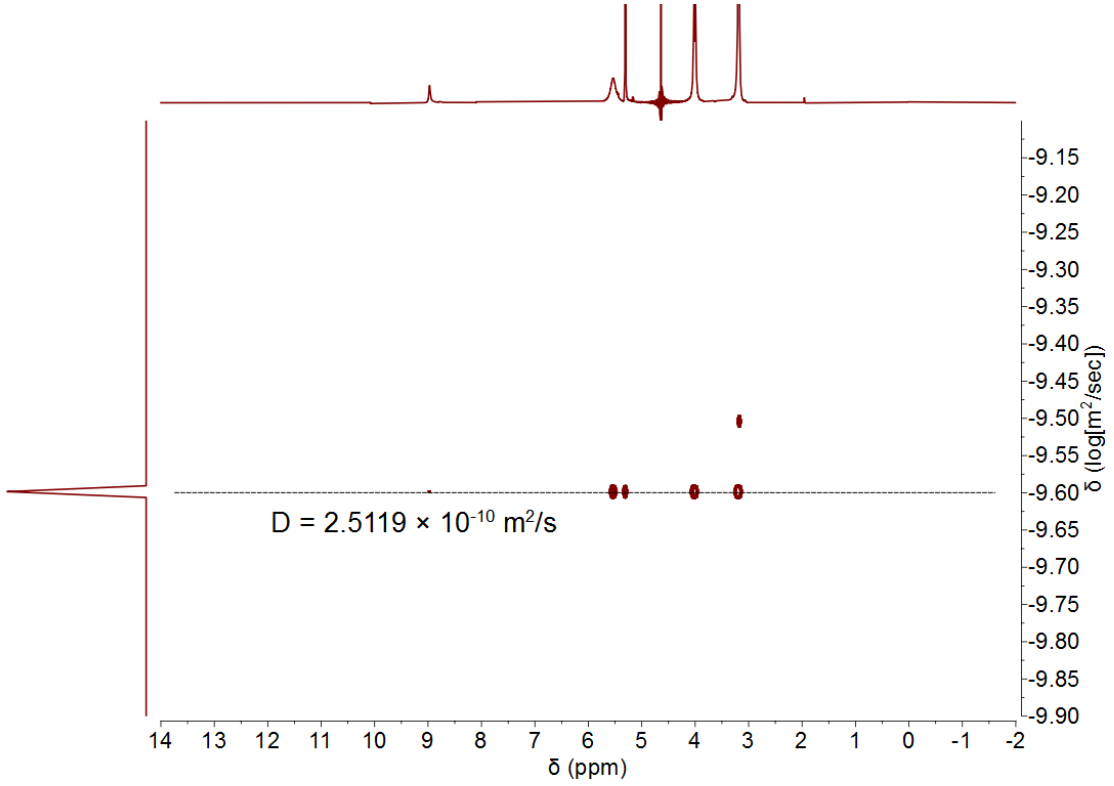

Figure S20. DOSY of 8.0 mM 2Br-NDI in the presence of 1.1 eq. CB[8] (hydrated diameter d_h = 1.9 nm).

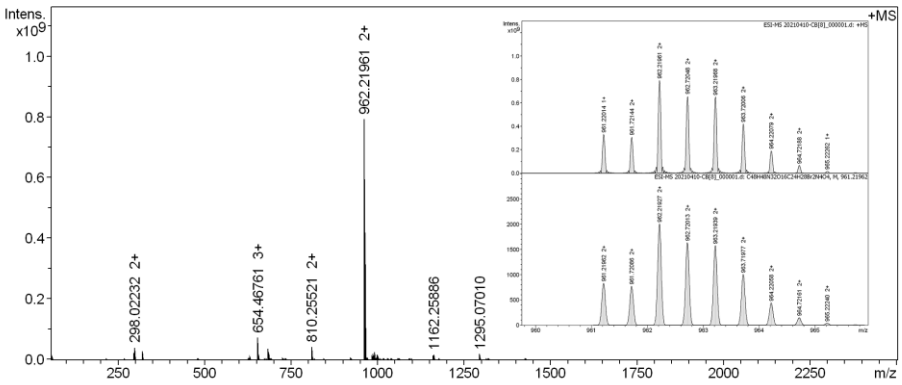

Figure S21. ESI-MS of the CB[8]·(2Br-NDI) complex (Inset: experimental (up) and predicted (down): m/z($C_{72}H_{76}Br_2N_{36}O_{20}^{2+}$): calc. = 962.21927, found = 962.21961, err. = 0.35 ppm for two positive charges.

CB[10]·(2Br-NDI)₂

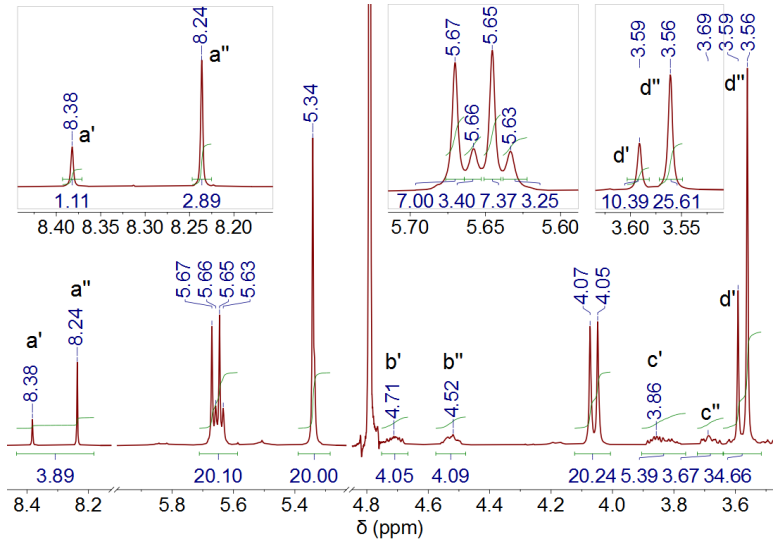

Figure S22. ^{1}H NMR (600 MHz, D_2O, 298 K) of the aqueous solution of CB[10]·$(2Br\text{-}NDI)_2$ complex ([2Br-NDI]= 5.0 mM).

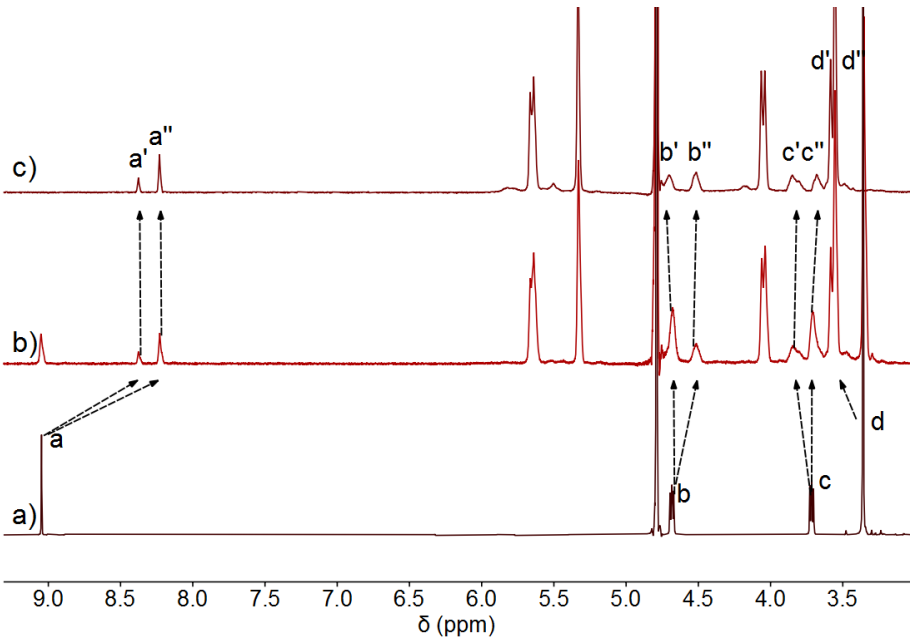

Figure S23. ^{1}H NMR (600 MHz, D_2O, 298 K) of 2.0 mM 2Br-NDI in the absence (a) and in the presence of 0.25 eq. (b) and 0.5 eq. (c) CB[10].

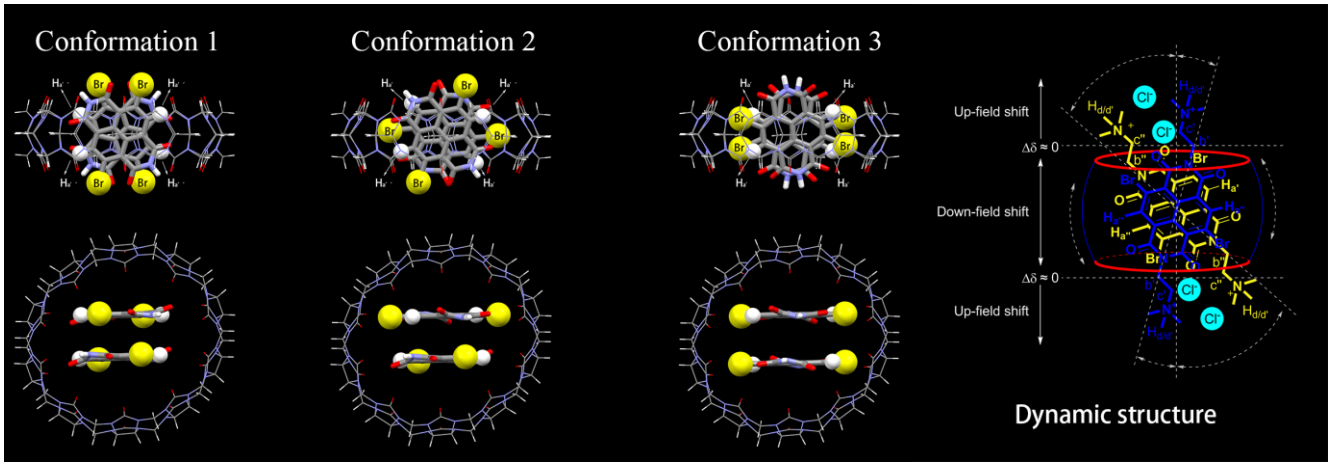

Figure S24. Conformations analysis of the CB[10]·(2Br-ND)$_2$ complex. Three conformations could be speculated for CB[10]·(2Br-NDI)$_2$. Among them, conformation 1 presents the least steric hindrance with the aromatic protons in the deeper cavity of CB[10]; aromatic protons in conformation 3 undergo less up-field shift due to the large steric hindrance from the inside bromine atoms. The symmetrical conformation-1 and conformation-3 were excluded because neither of them will arouse chemical shift splitting for H_a. Compromisingly, conformation-2 positioned two of the bromine atoms inside but the other two out of the cavity of CB[10] and resulted in different surroundings and signals splitting of the aromatic protons. In combined with the ^{1}H NMR integral ratio of $H_{a'}$: $H_{a''}$ ≈ 1:3 in Figure S22, the 2Br-NDI homodimer could be slipped along the central axis of CB[10].

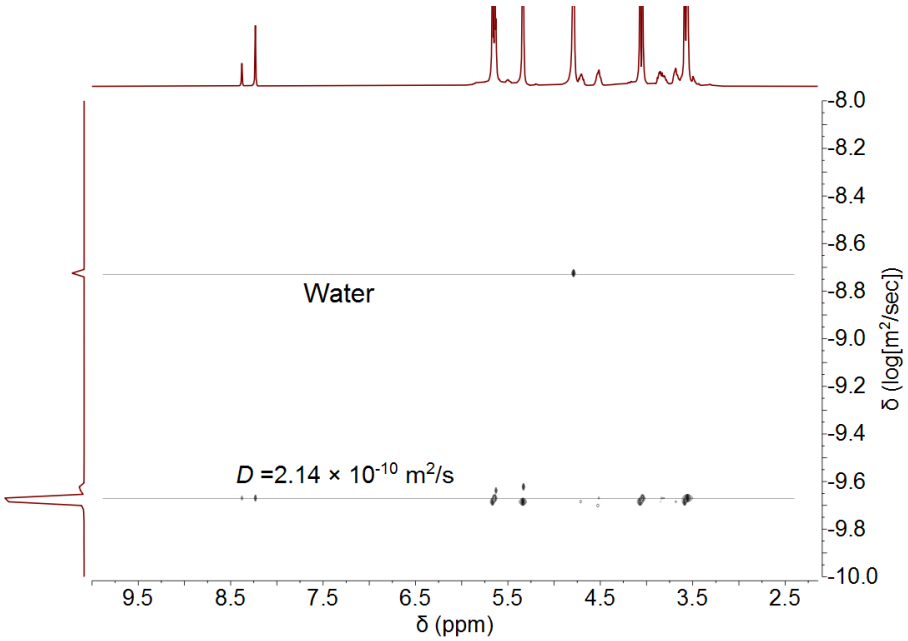

Figure S25. DOSY (600 MHz, D_2O, 298K) of the CB[10]·(2Br-NDI)$_2$ complex ([2Br-NDI] = 5.0 mM, hydrated diameter d_h = 2.2 nm).

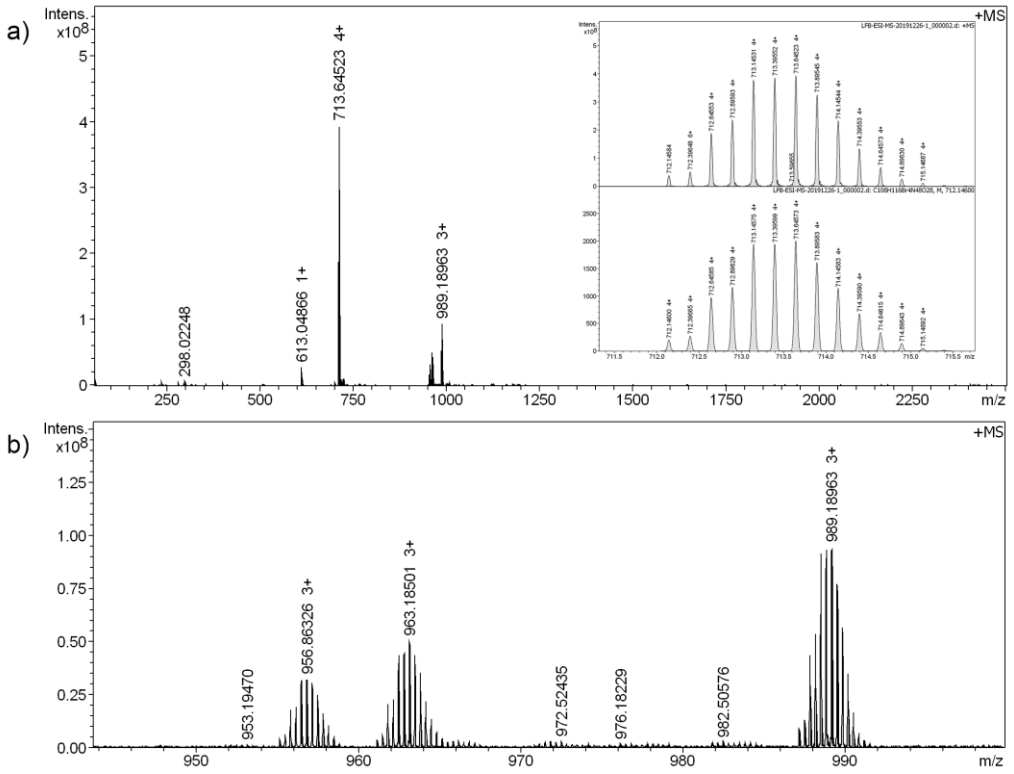

Figure S26. a) Full and b) partial view ESI-MS of the CB[10]·(2Br-NDI)$_2$ complex (Inset in full view: experimental (up) and predicted (down) ESI-MS of the CB[10]·(2Br-NDI)$_2$ complex; m/z($C_{108}H_{116}Br_4N_{48}O_{28}^{4+}$): calc. = 713.64573, found = 713.64523, err. = -0.7 ppm for four positive charges).

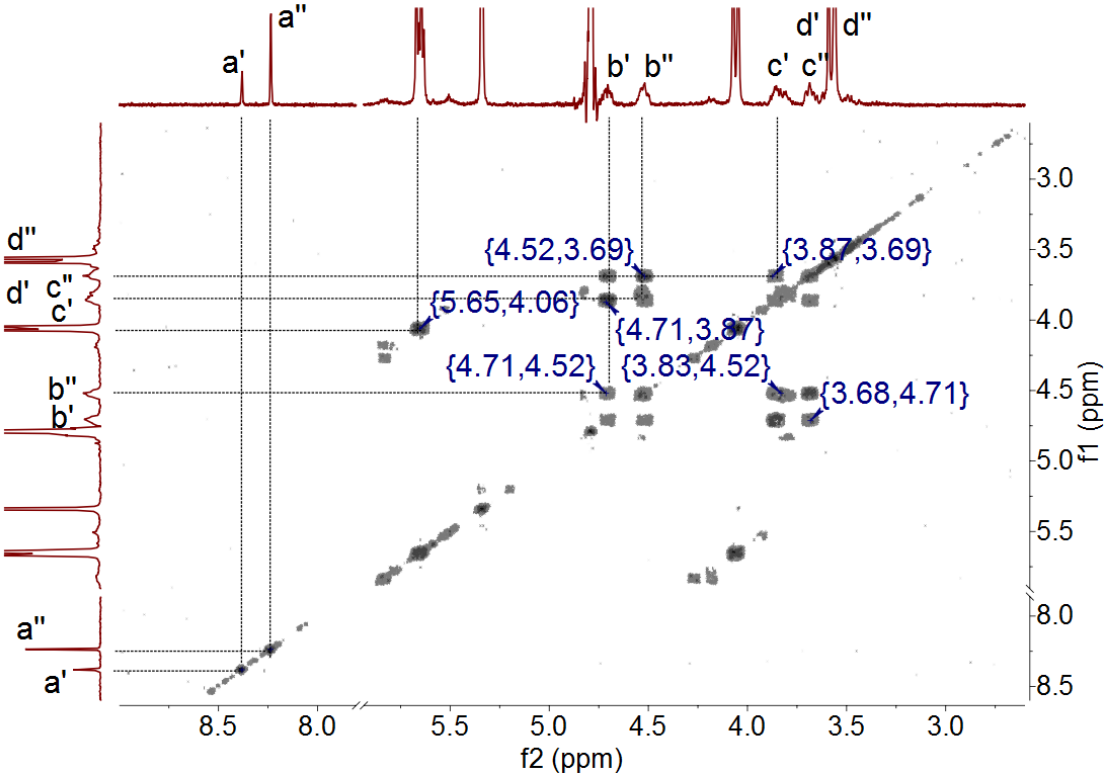

Figure S27. COSY (600 MHz, D_2O, 298 K) of the CB[10]·(2Br-NDI)$_2$ complex ([2Br-NDI]= 5.0 mM).

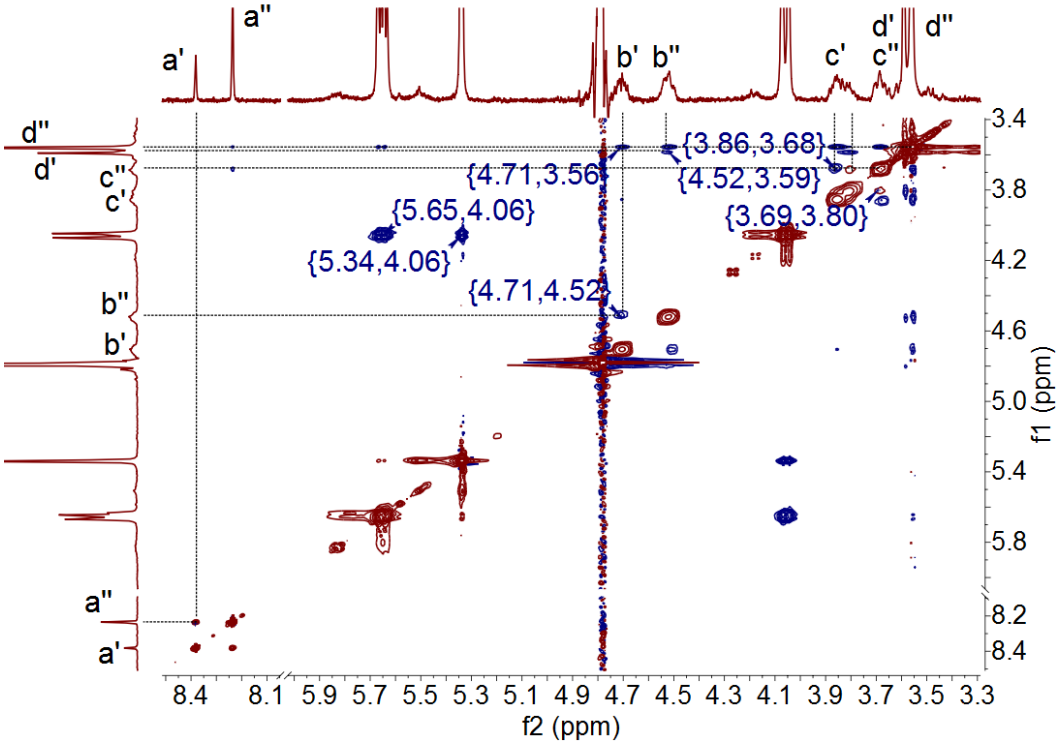

Figure S28. ^{1}H-^{1}H ROESY (600 MHz, D_2O, 298 K) of the CB[10]·(2Br-NDI)$_2$ complex ([2Br-NDI] = 5.0 mM). (Mixing time = 300 ms).

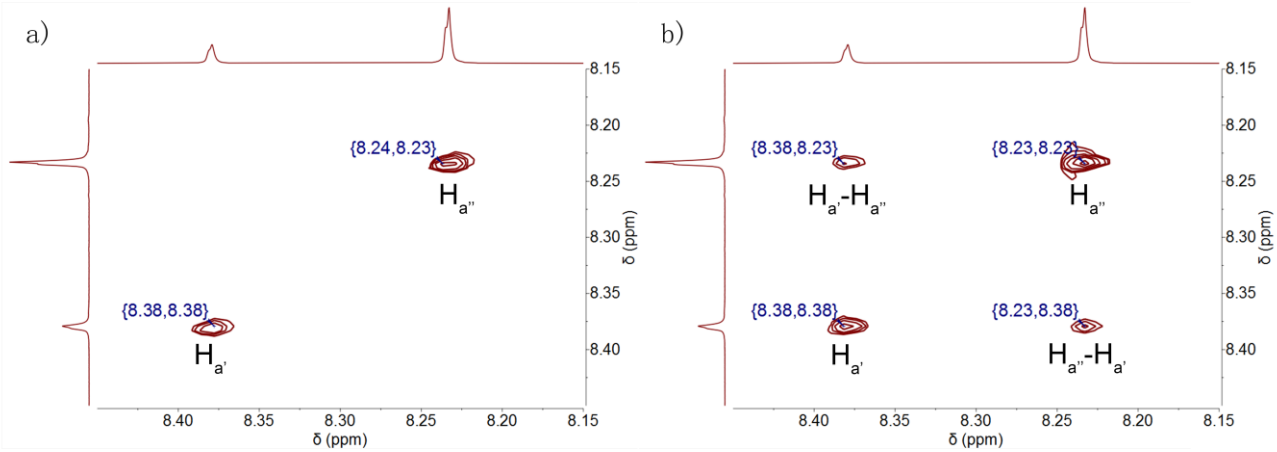

Figure S29. ROESY spectra of the CB[10]·(2Br-NDI)$_2$ ([2Br-NDI] = 6.6 mM) with the mixing time at a) 0 ms and b) 500 ms. The magnetization exchange rate constants were estimated as $k_{1'}$ = 0.220 s^{-1} and $k_{-1'}$ = 0.583 s^{-1}, respectively.

UV-Vis spectra and DLS change of 2Br-NDI upon addition of CB[*n*]s (*n* = 7, 8, 10)

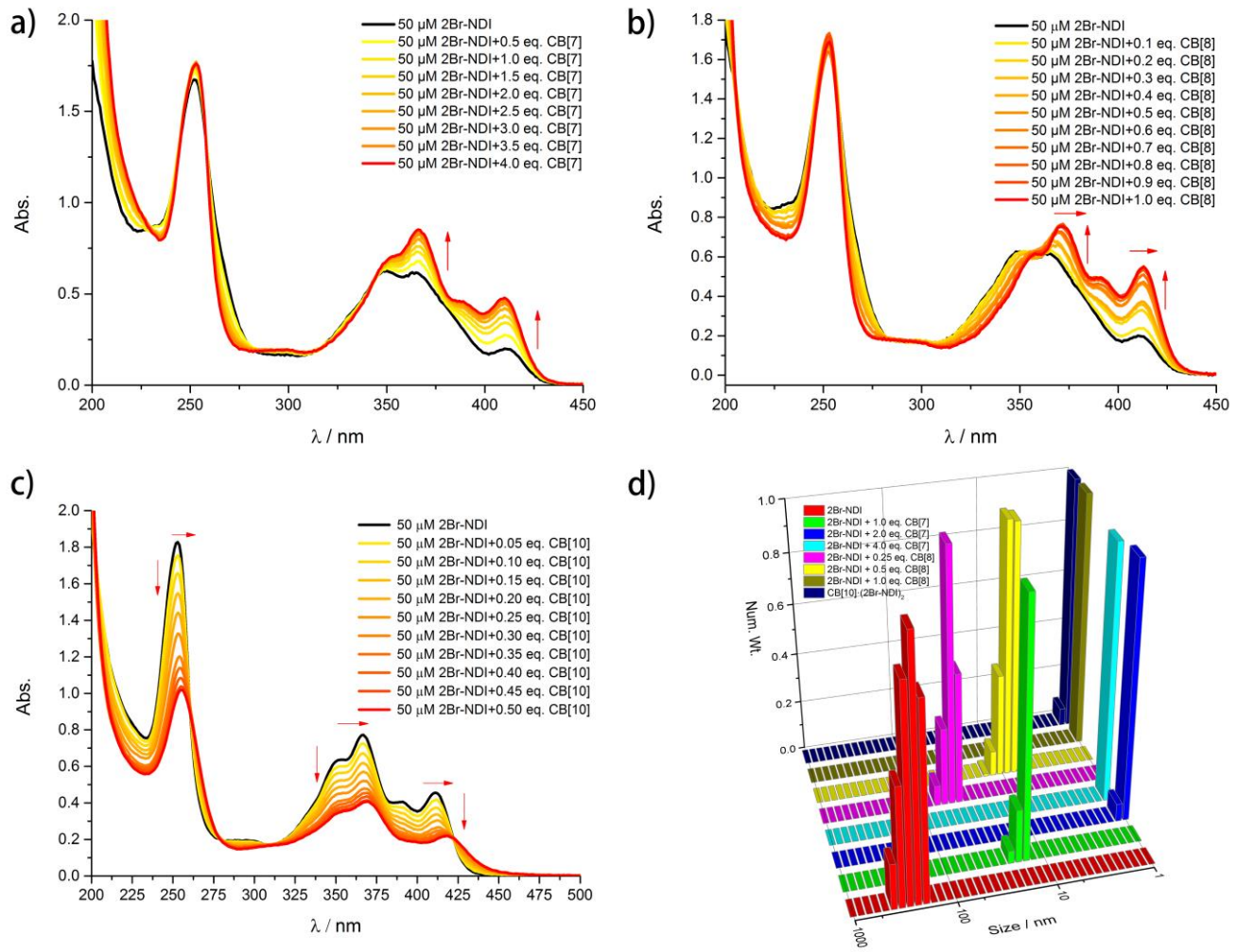

Figure S30. UV-Vis titration of 50 μM 2Br-NDI upon addition of a) CB[7], b) CB[8] and c) CB[10]. d) Size (NICOMP Number weighting) changing of the aqueous 125 μM 2Br-NDI solution upon addition of CB[*n*]s (*n* = 7, 8, 10).

Steady and gated emission of 2Br-NDI and its complexes with CB[*n*]s (*n* = 7, 8, 10)

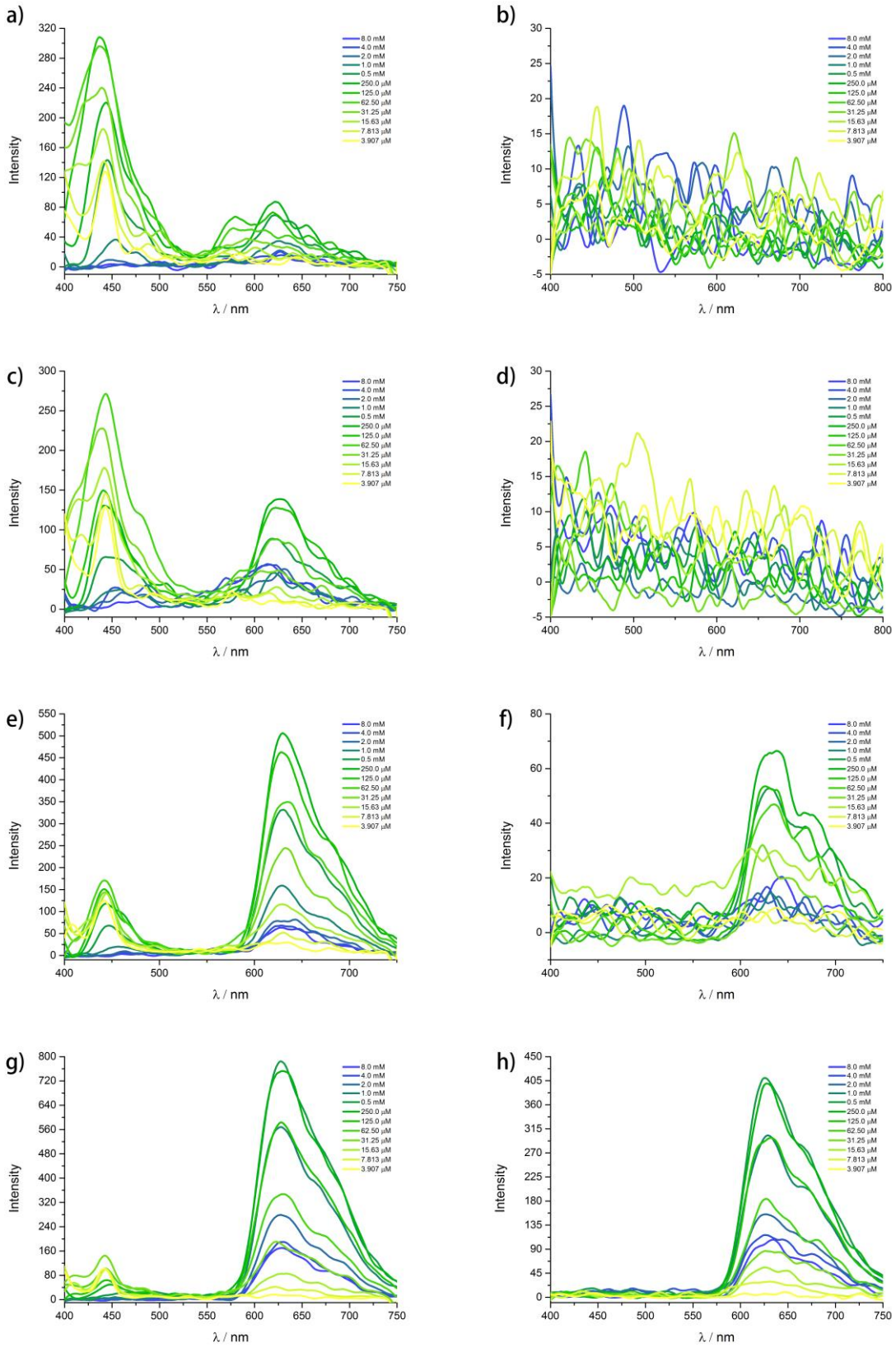

Figure S31. Steady (a, c, e, g) and gated (b, d, f, h) emission of 2Br-NDI in air in the absence (a & b) and presence of excess CB[7] (c & d), 1.0 eq. CB[8] (e & f) and 0.5 eq. CB[10] (g & h) at various concentrations (λ_{Ex} = 385 nm, $Slit_{Ex}$=3.5 nm, $Slit_{Em}$=12.5 nm; τ_{delay}=0.06 ms, τ_{gated}=0.04 ms).

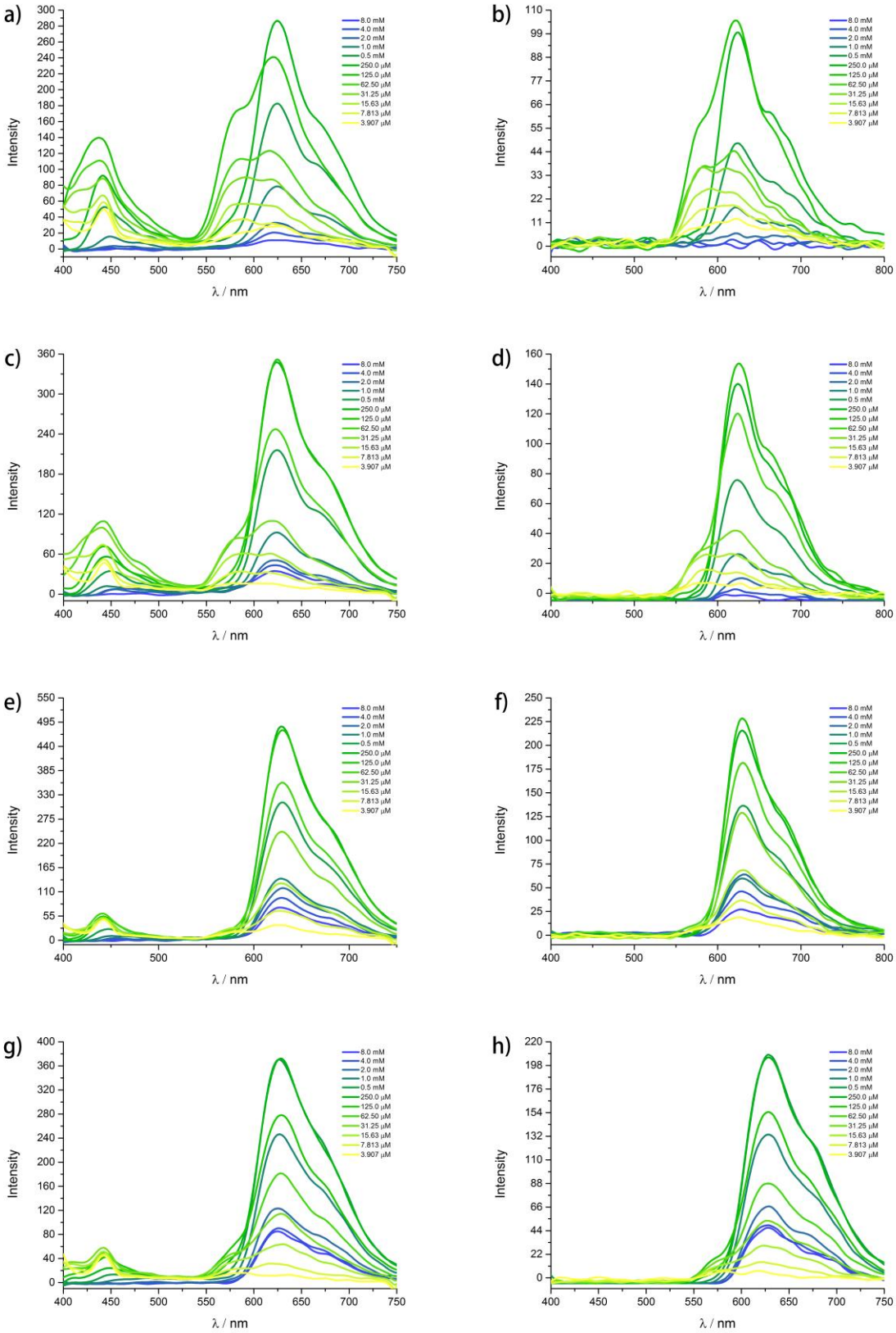

Figure S32. Steady (a, c, e, g) and gated (b, d, f, h) emission of 2Br-NDI in N_2 in the absence (a & b) and presence of excess CB[7] (c & d), 1.0 eq. CB[8] (e & f) and 0.5 eq. CB[10] (g & h) at various concentrations (λ_{Ex} = 385 nm, $Slit_{Ex}$ = 6 nm, $Slit_{Em}$= 10 nm; τ_{delay}=0.06 ms, τ_{gated}=0.04 ms).

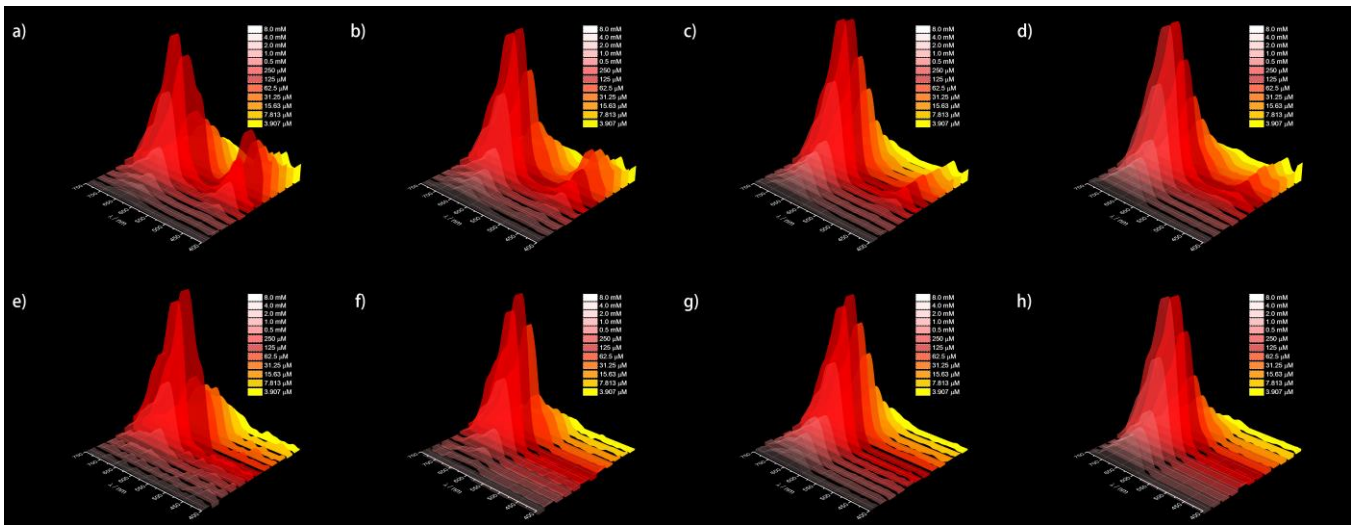

Figure S33. 3D views for the steady (a, b, c, d) and gated (e, f, g, h) emission of 2Br-NDI in N_2 in the absence (a & e) and presence of excess CB[7] (b & f), 1.0 eq. CB[8] (c & g) and 0.5 eq. CB[10] (d & h) at various concentrations. (λ_{Ex} = 385 nm, $slit_{Ex}$= 6.0 nm, $slit_{Em}$=10 nm, τ_{delay}=0.06 ms, τ_{gated}=0.04 ms).

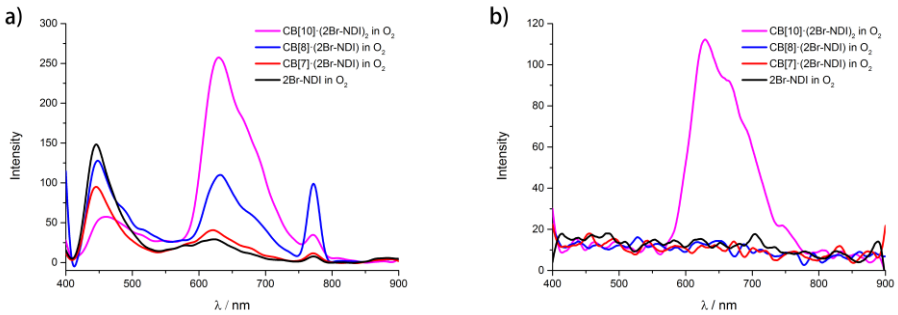

Figure S34. a) Steady ($slit_{Ex}$=7.5 nm, $slit_{Em}$=15.0 nm) and b) gated ($slit_{Ex}$=4.0 nm, $slit_{Em}$=15.0 nm, t_{delay}= 60 μs, t_{gate}=40 μs) emission of 333 μM 2Br-NDI in the absence and presence of CB[*n*]s (*n* = 7, 8, 10) in O_2 environment (λ_{Ex} = 385 nm).

Fluorescent and phosphorescent quantum yields measurements

2Br-NDI

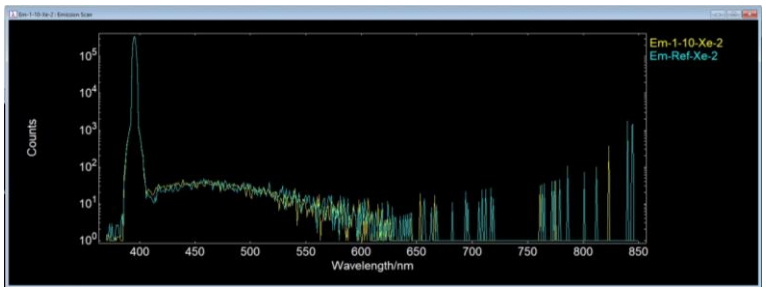

Figure S35. Fluorescent quantum yield of 2Br-NDI (15.6 μM).

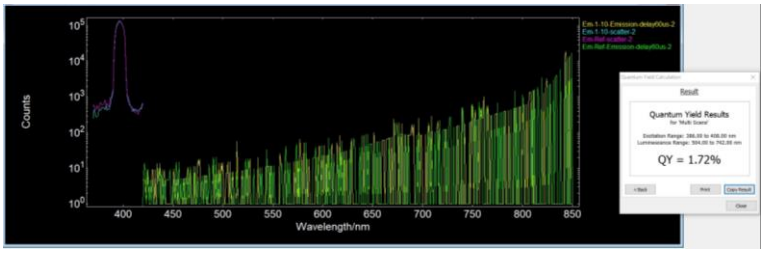

Figure S36. Phosphorescent quantum yield of 2Br-NDI (15.6 μM).

(CB[7])$_2$·(2Br-NDI)

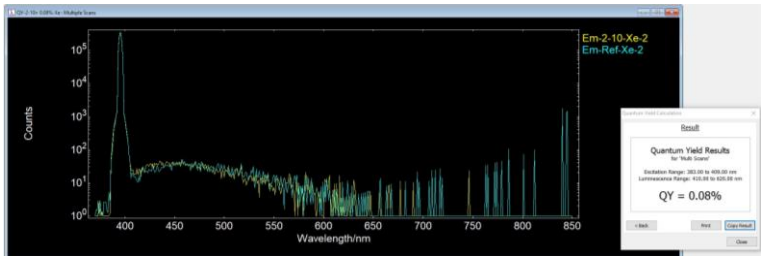

Figure S37. Fluorescent quantum yield of the (CB[7])$_2$•(2Br-NDI) complex ([2Br-NDI] = 15.6 μM).

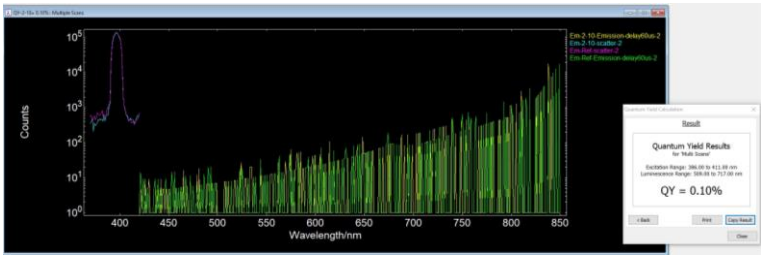

Figure S38. Phosphorescent quantum yield of the (CB[7])$_2$•(2Br-NDI) complex ([2Br-NDI] = 15.6 μM).

CB[8]·(2Br-NDI)

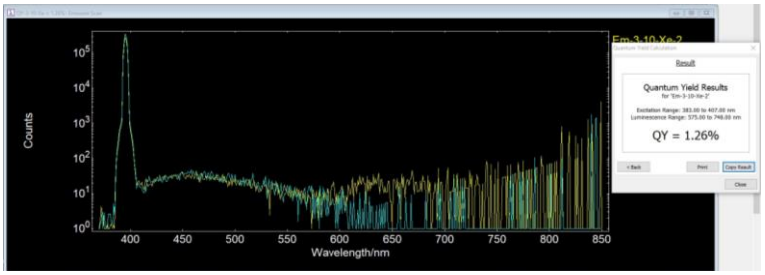

Figure S39. Fluorescent quantum yield of the CB[8]•(2Br-NDI) complex ([2Br-NDI] = 15.6 μM).

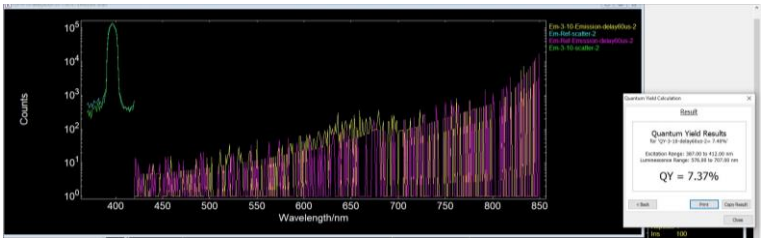

Figure S40. Phosphorescent quantum yield of the CB[8]•(2Br-NDI) complex ([2Br-NDI] = 15.6 μM).

CB[10]·(2Br-NDI)$_2$

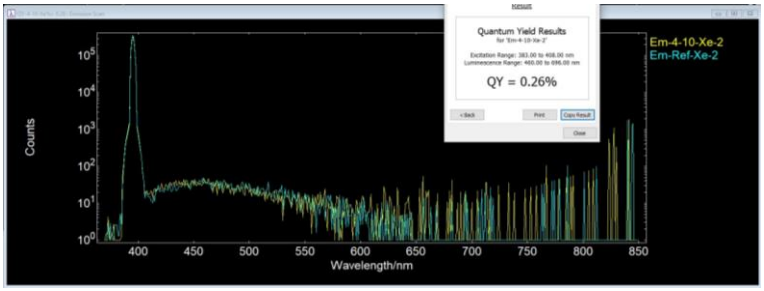

Figure S41. Fluorescent quantum yield of the CB[10]•(2Br-NDI)$_2$ complex ([2Br-NDI] = 15.6 μM).

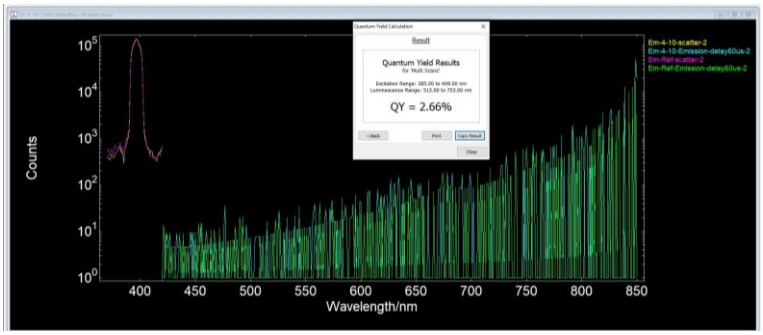

Figure S42. Phosphorescent quantum yield of the CB[10]•(2Br-NDI)$_2$ complex ([2Br-NDI] = 15.6 μM).

Steady emission-excitation spectra

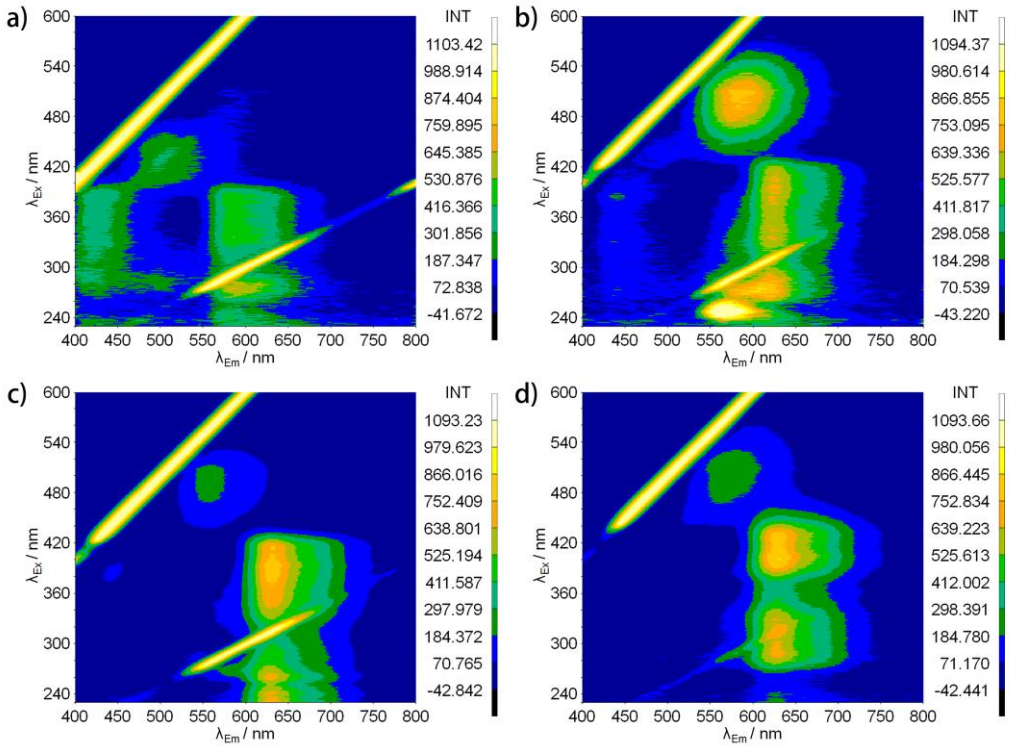

Figure S43. Steady emission-excitation spectra of 2Br-NDI in the absence (a) and presence of excess CB[7] (b), 1.0 eq. CB[8] (c), and 0.5 eq. CB[10] (d) in N_2.

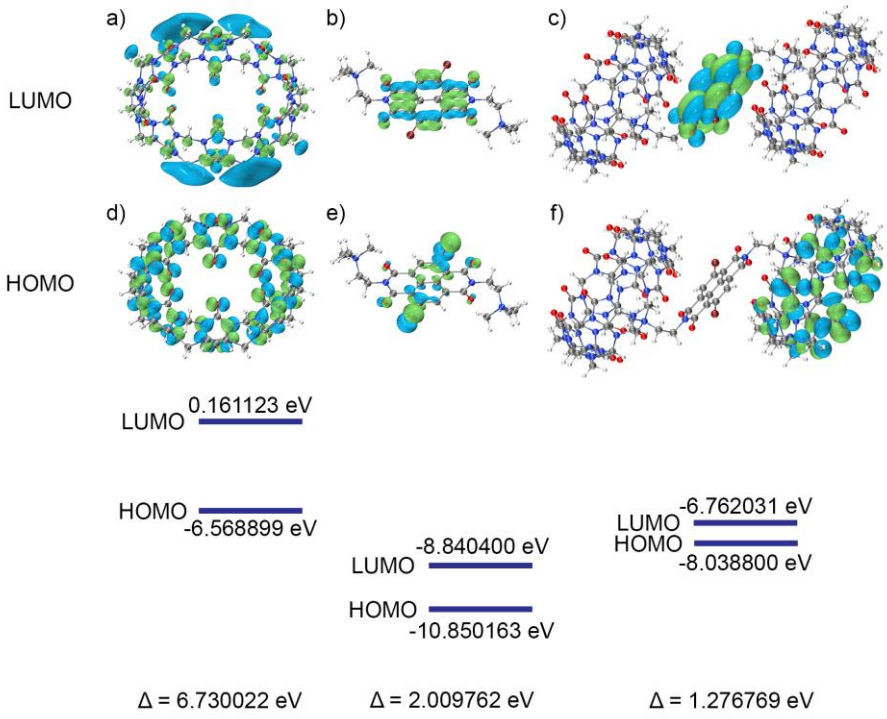

Figure S44. Orbital energy level analyses of CB[8] (a & d), 2Br-NDI (b & e) and the CB[8]·(2Br-NDI) complex (e & f).

Single crystal data

2Br-NDI

Table S2. Crystal data and structure refinement for 2Br-NDI.

Identification code	1_a	
Empirical formula	C24 H40 Br2 Cl2 N4 O10	
Formula weight	775.32	
Temperature	296(2) K	
Wavelength	0.71073 Å	
Crystal system	Triclinic	
Space group	P-1	
Unit cell dimensions	a = 6.6366(19) Å	a= 82.484(7)°.
	b = 6.8219(19) Å	b= 87.519(7)°.
	c = 19.554(6) Å	g = 68.781(6)°.
Volume	818.2(4) Å3	
Z	1	
Density (calculated)	1.574 Mg/m3	
Absorption coefficient	2.696 mm-1	
F(000)	396	
Crystal size	0.220 x 0.200 x 0.180 mm3	
Theta range for data collection	3.153 to 25.079°.	
Index ranges	-7<=h<=7, -8<=k<=7, -23<=l<=23	
Reflections collected	22445	
Independent reflections	2878 [R(int) = 0.0875]	
Completeness to theta = 25.079°	99.30%	
Absorption correction	Semi-empirical from equivalents	
Refinement method	Full-matrix least-squares on F2	
Data / restraints / parameters	2878 / 0 / 190	
Goodness-of-fit on F2	1.071	
Final R indices [I>2sigma(I)]	R1 = 0.0637, wR2 = 0.1652	
R indices (all data)	R1 = 0.0934, wR2 = 0.1803	
Extinction coefficient	n/a	
Largest diff. peak and hole	0.924 and -0.631 e.Å-3	

Table S3. Atomic coordinates (x 10^4) and equivalent isotropic displacement parameters ($Å^2$x 10^3) for 2Br-NDI. U(eq) is defined as one third of the trace of the orthogonalized U^{ij} tensor.

	x	y	z	U(eq)
Br(1)	5588(1)	1578(1)	5623(1)	43(1)
C(1)	12321(10)	5787(10)	4035(3)	36(2)
C(2)	10990(10)	4629(9)	4112(3)	33(2)
C(3)	9884(9)	4438(9)	4726(3)	30(1)
C(4)	8517(10)	3235(9)	4805(3)	33(2)
C(5)	7466(10)	3112(10)	5423(3)	34(2)
C(6)	8334(12)	2101(10)	4224(4)	42(2)
C(7)	10843(11)	3506(11)	3524(4)	41(2)
C(8)	9478(12)	999(11)	3089(4)	43(2)
C(9)	7359(12)	1997(12)	2675(4)	46(2)
C(10)	8935(18)	3254(17)	1618(5)	81(3)
C(11)	5496(15)	2760(16)	1583(5)	71(3)
C(12)	8799(16)	-317(15)	1767(5)	77(3)
N(1)	9552(9)	2284(8)	3631(3)	38(1)
N(2)	7698(10)	1904(10)	1910(3)	50(2)
O(1)	11754(10)	3641(10)	2981(3)	66(2)
O(2)	7229(10)	1039(10)	4229(3)	70(2)
Cl(1)	4560(4)	7827(4)	2377(1)	71(1)
O(3)	3994(12)	8461(11)	826(3)	100(2)
O(4)	1731(15)	6370(14)	377(3)	167(5)
O(5)	2541(12)	2307(12)	10030(3)	104(2)

Table S4. Bond lengths [Å] and angles [°] for 2Br-NDI. (Symmetry transformations used to generate equivalent atoms: #1 -x+2,-y+1,-z+1)

Br(1)-C(5)	1.896(6)	C(4)-C(5)-C(1)#1	121.1(6)
C(1)-C(2)	1.375(9)	C(4)-C(5)-Br(1)	124.6(5)
C(1)-C(5)#1	1.417(9)	C(1)#1-C(5)-Br(1)	114.2(5)
C(1)-H(1)	0.93	O(2)-C(6)-N(1)	118.1(6)
C(2)-C(3)	1.396(9)	O(2)-C(6)-C(4)	124.6(7)
C(2)-C(7)	1.487(10)	N(1)-C(6)-C(4)	117.3(6)
C(3)-C(4)	1.420(9)	O(1)-C(7)-N(1)	121.0(6)
C(3)-C(3)#1	1.441(13)	O(1)-C(7)-C(2)	123.3(6)
C(4)-C(5)	1.376(9)	N(1)-C(7)-C(2)	115.7(6)
C(4)-C(6)	1.488(10)	N(1)-C(8)-C(9)	111.5(5)
C(5)-C(1)#1	1.417(10)	N(1)-C(8)-H(8A)	109.3
C(6)-O(2)	1.201(8)	C(9)-C(8)-H(8A)	109.3
C(6)-N(1)	1.402(9)	N(1)-C(8)-H(8B)	109.3
C(7)-O(1)	1.208(9)	C(9)-C(8)-H(8B)	109.3
C(7)-N(1)	1.389(9)	H(8A)-C(8)-H(8B)	108
C(8)-N(1)	1.475(8)	N(2)-C(9)-C(8)	112.7(6)
C(8)-C(9)	1.535(10)	N(2)-C(9)-H(9A)	109.1
C(8)-H(8A)	0.97	C(8)-C(9)-H(9A)	109.1
C(8)-H(8B)	0.97	N(2)-C(9)-H(9B)	109.1
C(9)-N(2)	1.510(9)	C(8)-C(9)-H(9B)	109.1
C(9)-H(9A)	0.97	H(9A)-C(9)-H(9B)	107.8
C(9)-H(9B)	0.97	N(2)-C(10)-H(10A)	109.5
C(10)-N(2)	1.489(11)	N(2)-C(10)-H(10C)	109.5
C(10)-H(10A)	0.96	H(10A)-C(10)-H(10C)	109.5
C(10)-H(10C)	0.96	N(2)-C(10)-H(10B)	109.5
C(10)-H(10B)	0.96	H(10A)-C(10)-H(10B)	109.5
C(11)-N(2)	1.501(10)	H(10C)-C(10)-H(10B)	109.5
C(11)-H(11A)	0.96	N(2)-C(11)-H(11A)	109.5
C(11)-H(11B)	0.96	N(2)-C(11)-H(11B)	109.5
C(11)-H(11C)	0.96	H(11A)-C(11)-H(11B)	109.5
C(12)-N(2)	1.484(11)	N(2)-C(11)-H(11C)	109.5
C(12)-H(12B)	0.96	H(11A)-C(11)-H(11C)	109.5
C(12)-H(12C)	0.96	H(11B)-C(11)-H(11C)	109.5
C(12)-H(12A)	0.96	N(2)-C(12)-H(12B)	109.5
O(3)-H(3A)	0.8501	N(2)-C(12)-H(12C)	109.5
O(3)-H(3B)	0.8503	H(12B)-C(12)-H(12C)	109.5
O(4)-H(4A)	0.85	N(2)-C(12)-H(12A)	109.5
O(4)-H(4B)	0.8499	H(12B)-C(12)-H(12A)	109.5
O(5)-H(5A)	0.85	H(12C)-C(12)-H(12A)	109.5
O(5)-H(5B)	0.8499	C(7)-N(1)-C(6)	125.9(6)
C(2)-C(1)-C(5)#1	120.0(6)	C(7)-N(1)-C(8)	118.2(6)
C(2)-C(1)-H(1)	120	C(6)-N(1)-C(8)	115.9(5)
C(5)#1-C(1)-H(1)	120	C(12)-N(2)-C(10)	111.0(7)
C(1)-C(2)-C(3)	121.7(6)	C(12)-N(2)-C(11)	108.7(7)
C(1)-C(2)-C(7)	117.3(6)	C(10)-N(2)-C(11)	108.8(7)
C(3)-C(2)-C(7)	121.0(6)	C(12)-N(2)-C(9)	110.6(6)
C(2)-C(3)-C(4)	121.5(6)	C(10)-N(2)-C(9)	110.9(6)
C(2)-C(3)-C(3)#1	117.8(7)	C(11)-N(2)-C(9)	106.7(6)
C(4)-C(3)-C(3)#1	120.6(7)	H(3A)-O(3)-H(3B)	104.5
C(5)-C(4)-C(3)	118.8(6)	H(4A)-O(4)-H(4B)	104.5
C(5)-C(4)-C(6)	122.7(6)	H(5A)-O(5)-H(5B)	104.5
C(3)-C(4)-C(6)	118.5(6)		

Table S5. Anisotropic displacement parameters ($Å^2 x\ 10^3$) for 2Br-NDI. The anisotropic displacement factor exponent takes the form: $-2\pi^2[\ h^2a^{*2}U^{11} + ...\ + 2hka^*b^*U^{12}]$

	U11	U22	U33	U23	U13	U12
Br(1)	38(1)	43(1)	57(1)	0(1)	0(1)	-27(1)
C(1)	31(3)	38(4)	42(4)	-3(3)	4(3)	-17(3)
C(2)	32(3)	27(3)	42(4)	-2(3)	-4(3)	-12(3)
C(3)	21(3)	23(3)	43(4)	-1(3)	-3(3)	-6(2)
C(4)	32(3)	27(3)	42(4)	-1(3)	-3(3)	-12(3)
C(5)	26(3)	31(3)	48(4)	3(3)	-2(3)	-17(3)
C(6)	47(4)	34(4)	49(4)	-4(3)	-1(3)	-21(3)
C(7)	39(4)	43(4)	48(5)	-7(3)	0(3)	-21(3)
C(8)	48(4)	34(4)	48(4)	-11(3)	-2(3)	-13(3)
C(9)	43(4)	47(4)	49(4)	-9(3)	0(3)	-17(3)
C(10)	98(8)	104(8)	60(6)	13(5)	-2(5)	-66(7)
C(11)	69(6)	90(7)	59(5)	-4(5)	-17(5)	-34(5)
C(12)	78(7)	84(7)	77(7)	-41(5)	1(5)	-26(5)
N(1)	39(3)	35(3)	43(3)	-8(3)	-1(3)	-17(3)
N(2)	50(4)	59(4)	45(4)	-10(3)	-6(3)	-22(3)
O(1)	85(4)	92(4)	50(3)	-26(3)	23(3)	-63(4)
O(2)	93(5)	91(4)	67(4)	-30(3)	20(3)	-80(4)
Cl(1)	76(2)	61(1)	74(2)	-12(1)	15(1)	-24(1)
O(3)	106(6)	100(6)	97(6)	-2(4)	3(4)	-43(5)
O(4)	136(9)	132(8)	219(12)	-72(8)	-70(8)	-7(7)
O(5)	85(5)	99(6)	106(6)	-5(4)	4(4)	-10(4)

Table S6. Hydrogen coordinates (x 10^4) and isotropic displacement parameters ($Å^2$x 10^3) for 2Br-NDI.

	x	y	z	U(eq)
H(1)	13080	5849	3626	43
H(8A)	9615	-413	3299	52
H(8B)	10689	870	2779	52
H(9A)	6390	1263	2839	55
H(9B)	6674	3465	2757	55
H(10A)	10293	2808	1856	122
H(10C)	8119	4707	1673	122
H(10B)	9190	3119	1136	122
H(11A)	4829	4241	1628	107
H(11B)	4622	2014	1808	107
H(11C)	5627	2570	1103	107
H(12B)	8945	-352	1277	116
H(12C)	7960	-1150	1952	116
H(12A)	10205	-887	1978	116
H(3A)	3272	7765	699	150
H(3B)	4226	8036	1254	150
H(4A)	1850	5338	157	251
H(4B)	432	7211	307	251
H(5A)	2921	1303	10360	156
H(5B)	3490	1901	9721	156

Table S7. Torsion angles [°] for 2Br-NDI.

C(5)#1-C(1)-C(2)-C(3)	-2.3(10)
C(5)#1-C(1)-C(2)-C(7)	-179.8(6)
C(1)-C(2)-C(3)-C(4)	-179.8(6)
C(7)-C(2)-C(3)-C(4)	-2.4(9)
C(1)-C(2)-C(3)-C(3)#1	2.2(10)
C(7)-C(2)-C(3)-C(3)#1	179.6(6)
C(2)-C(3)-C(4)-C(5)	-179.8(6)
C(3)#1-C(3)-C(4)-C(5)	-1.9(10)
C(2)-C(3)-C(4)-C(6)	2.1(9)
C(3)#1-C(3)-C(4)-C(6)	-180.0(7)
C(3)-C(4)-C(5)-C(1)#1	2.0(9)
C(6)-C(4)-C(5)-C(1)#1	180.0(6)
C(3)-C(4)-C(5)-Br(1)	-179.8(4)
C(6)-C(4)-C(5)-Br(1)	-1.8(9)
C(5)-C(4)-C(6)-O(2)	2.1(11)
C(3)-C(4)-C(6)-O(2)	-179.9(7)
C(5)-C(4)-C(6)-N(1)	-177.5(6)
C(3)-C(4)-C(6)-N(1)	0.5(9)
C(1)-C(2)-C(7)-O(1)	-3.2(10)
C(3)-C(2)-C(7)-O(1)	179.3(7)
C(1)-C(2)-C(7)-N(1)	177.5(6)
C(3)-C(2)-C(7)-N(1)	0.0(9)
N(1)-C(8)-C(9)-N(2)	138.0(6)
O(1)-C(7)-N(1)-C(6)	-176.5(7)
C(2)-C(7)-N(1)-C(6)	2.8(10)
O(1)-C(7)-N(1)-C(8)	5.5(10)
C(2)-C(7)-N(1)-C(8)	-175.3(5)
O(2)-C(6)-N(1)-C(7)	177.3(7)
C(4)-C(6)-N(1)-C(7)	-3.1(10)
O(2)-C(6)-N(1)-C(8)	-4.6(10)
C(4)-C(6)-N(1)-C(8)	175.0(6)
C(9)-C(8)-N(1)-C(7)	-104.5(7)
C(9)-C(8)-N(1)-C(6)	77.3(7)
C(8)-C(9)-N(2)-C(12)	57.2(8)
C(8)-C(9)-N(2)-C(10)	-66.4(8)
C(8)-C(9)-N(2)-C(11)	175.3(6)

Symmetry transformations used to generate equivalent atoms:
#1 -x+2,-y+1,-z+1

CB[8]·(2Br-NDI)

Table S8. Crystal data and structure refinement for CB[8]•[2Br-NDI]

Identification code	CB[8]•[2Br-NDI]	
Empirical formula	C72 H108 Br2 I2 N36 O36	
Formula weight	2467.56	
Temperature	150(2) K	
Wavelength	0.71073 Å	
Crystal system	Monoclinic	
Space group	$P2_1/n$	
Unit cell dimensions	a = 14.3431(18) Å	α= 90°.
	b = 16.633(2) Å	β= 97.151(4)°.
	c = 20.226(3) Å	γ = 90°.
Volume	4787.8(11) $Å^3$	
Z	2	
Density (calculated)	1.712 Mg/m^3	
Absorption coefficient	1.597 mm^{-1}	
F(000)	2512	
Crystal size	0.200 x 0.200 x 0.200 mm^3	
Theta range for data collection	1.648 to 26.422°.	
Index ranges	-17<=h<=17, -20<=k<=20, -25<=l<=25	
Reflections collected	65954	
Independent reflections	9738 [R(int) = 0.0472]	
Completeness to theta = 25.242°	99.4 %	
Absorption correction	Semi-empirical from equivalents	
Refinement method	Full-matrix least-squares on F^2	
Data / restraints / parameters	9738 / 24 / 712	
Goodness-of-fit on F^2	1.171	
Final R indices [I>2sigma(I)]	R1 = 0.0339, wR2 = 0.0860	
R indices (all data)	R1 = 0.0354, wR2 = 0.0867	
Extinction coefficient	n/a	
Largest diff. peak and hole	0.989 and -1.241 e.$Å^{-3}$	

Table S9. Atomic coordinates (x 10^4) and equivalent isotropic displacement parameters ($Å^2$x10^3) for CB[8]•[2Br-NDI]. U(eq) is defined as one third of the trace of the orthogonalized U^{ij} tensor.

	x	y	z	U(eq)		x	y	z	U(eq)
Br(1)	5470(1)	9747(1)	2894(1)	27(1)	I(1)	1904(1)	355(1)	5025(1)	19(1)
C(1)	6645(2)	7793(1)	4914(1)	14(1)	N(1)	7204(2)	7651(1)	5509(1)	14(1)
C(2)	8138(2)	7392(1)	5406(1)	13(1)	N(2)	7133(2)	7547(1)	4400(1)	14(1)
C(3)	8091(2)	7328(1)	4636(1)	14(1)	N(3)	8364(2)	6582(1)	5636(1)	15(1)
C(4)	8545(2)	6084(2)	5120(1)	16(1)	N(4)	8314(2)	6493(1)	4529(1)	16(1)
C(5)	8749(2)	6420(2)	6320(1)	16(1)	N(5)	6677(2)	7166(1)	3254(1)	16(1)
C(6)	6855(2)	7821(2)	3722(1)	17(1)	N(6)	5932(2)	6519(1)	2382(1)	14(1)
C(7)	8612(2)	6210(2)	3911(1)	17(1)	N(7)	7837(2)	6085(1)	3389(1)	16(1)
C(8)	5822(2)	7080(2)	2867(1)	15(1)	N(8)	7106(2)	5463(1)	2494(1)	14(1)
C(9)	7422(2)	6743(2)	2976(1)	14(1)	N(9)	4807(2)	5641(1)	1768(1)	14(1)
C(10)	6899(2)	6305(1)	2361(1)	13(1)	N(10)	3704(2)	4729(1)	1866(1)	13(1)
C(11)	7696(2)	5354(1)	3072(1)	13(1)	N(11)	5951(2)	4546(1)	1930(1)	15(1)
C(12)	5245(2)	6426(1)	1807(1)	15(1)	N(12)	4823(2)	3624(1)	1847(1)	16(1)
C(13)	6912(2)	4842(2)	1994(1)	14(1)	N(13)	2469(2)	3970(1)	2288(1)	15(1)
C(14)	3960(2)	5515(2)	1991(1)	13(1)	N(14)	1963(2)	3570(1)	3230(1)	15(1)
C(15)	5189(2)	4925(2)	1502(1)	14(1)	N(15)	3709(2)	2960(1)	2482(1)	14(1)
C(16)	4375(2)	4310(1)	1506(1)	13(1)	N(16)	3061(2)	2448(1)	3332(1)	15(1)
C(17)	5749(2)	3757(2)	2073(1)	14(1)	N(17)	3647(2)	6479(1)	5728(1)	19(1)
C(18)	2720(2)	4514(2)	1785(1)	16(1)	N(18)	3469(2)	8457(1)	5381(1)	16(1)
C(19)	4333(2)	2889(2)	1966(1)	17(1)	O(1)	5857(1)	8071(1)	4854(1)	20(1)
C(20)	2058(2)	4226(2)	2823(1)	14(1)	O(2)	8834(2)	5398(1)	5174(1)	24(1)
C(21)	2713(2)	3126(1)	2313(1)	14(1)	O(3)	5094(1)	7422(1)	2950(1)	21(1)
C(22)	2277(2)	2828(2)	2936(1)	14(1)	O(4)	8040(1)	4713(1)	3279(1)	19(1)
C(23)	3879(2)	2505(1)	3055(1)	14(1)	O(5)	3500(1)	6020(1)	2246(1)	19(1)
C(24)	2966(2)	1923(2)	3893(1)	15(1)	O(6)	6304(1)	3268(1)	2342(1)	19(1)
C(25)	5322(2)	10292(2)	4916(1)	14(1)	O(7)	1802(1)	4910(1)	2927(1)	21(1)
C(26)	5575(2)	10350(2)	4260(1)	15(1)	O(8)	4630(1)	2206(1)	3279(1)	20(1)
C(27)	5187(2)	9803(2)	3783(1)	16(1)	O(9)	3244(2)	8095(1)	4286(1)	26(1)
C(28)	4546(2)	9217(2)	3945(1)	16(1)	O(10)	3454(1)	8941(1)	6420(1)	22(1)
C(29)	4290(2)	9175(2)	4576(1)	15(1)	O(11)	9672(2)	1262(1)	4933(1)	34(1)
C(30)	3630(2)	8536(2)	4720(1)	17(1)	O(12)	9632(2)	2880(2)	4646(2)	45(1)
C(31)	3758(2)	9013(2)	5890(1)	17(1)	O(13)	9211(2)	3835(1)	5673(2)	41(1)
C(32)	2805(2)	7837(2)	5550(1)	19(1)	O(14)	7884(2)	3556(1)	6534(2)	41(1)
C(33)	3255(2)	7210(2)	6042(1)	18(1)	O(15)	8766(2)	3077(1)	3342(2)	42(1)
C(34)	4362(2)	6709(2)	5284(2)	27(1)	O(16)	5946(2)	4114(2)	6313(1)	50(1)
C(35)	2870(2)	5997(2)	5345(2)	31(1)	O(17)	3658(2)	4404(2)	4276(2)	51(1)
C(36)	4111(2)	5966(2)	6285(1)	24(1)	O(18)	4090(2)	4090(2)	5652(1)	40(1)

Table S10. Bond lengths [Å] and angles [°] for CB[8]•[2Br-NDI].

Br(1)-C(27)	1.893(3)	C(11)-N(7)	1.378(3)	C(22)-N(14)	1.465(3)	C(35)-H(35C)	0.98
C(1)-O(1)	1.213(3)	C(12)-N(6)	1.436(3)	C(22)-H(22)	1	C(36)-N(17)	1.501(3)
C(1)-N(1)	1.382(3)	C(12)-N(9)	1.447(3)	C(23)-O(8)	1.221(3)	C(36)-H(36A)	0.98
C(1)-N(2)	1.385(3)	C(12)-H(12A)	0.99	C(23)-N(16)	1.366(3)	C(36)-H(36B)	0.98
C(2)-N(1)	1.446(3)	C(12)-H(12B)	0.99	C(23)-N(15)	1.381(3)	C(36)-H(36C)	0.98
C(2)-N(3)	1.450(3)	C(13)-N(8)	1.448(3)	C(24)-N(1)#1	1.448(3)	N(1)-C(24)#1	1.448(3)
C(2)-C(3)	1.554(3)	C(13)-N(11)	1.454(3)	C(24)-N(16)	1.451(3)	N(14)-C(5)#1	1.451(3)
C(2)-H(2)	1	C(13)-H(13A)	0.99	C(24)-H(24A)	0.99	O(11)-H(11D)	0.837(10)
C(3)-N(2)	1.444(3)	C(13)-H(13B)	0.99	C(24)-H(24B)	0.99	O(11)-H(11E)	0.838(10)
C(3)-N(4)	1.447(3)	C(14)-O(5)	1.220(3)	C(25)-C(25)#2	1.412(5)	O(12)-H(12D)	0.842(10)
C(3)-H(3)	1	C(14)-N(9)	1.364(3)	C(25)-C(29)#2	1.416(4)	O(12)-H(12E)	0.843(10)
C(4)-O(2)	1.215(3)	C(14)-N(10)	1.373(3)	C(25)-C(26)	1.423(4)	O(13)-H(13D)	0.843(10)
C(4)-N(4)	1.380(3)	C(15)-N(9)	1.443(3)	C(26)-C(27)	1.390(4)	O(13)-H(13E)	0.839(10)
C(4)-N(3)	1.380(3)	C(15)-N(11)	1.451(3)	C(26)-C(31)#2	1.484(4)	O(14)-H(14D)	0.843(10)
C(5)-N(3)	1.450(3)	C(15)-C(16)	1.553(3)	C(27)-C(28)	1.406(4)	O(14)-H(14E)	0.842(10)
C(5)-N(14)#1	1.451(3)	C(15)-H(15)	1	C(28)-C(29)	1.373(4)	O(15)-H(15D)	0.841(10)
C(5)-H(5A)	0.99	C(16)-N(12)	1.441(3)	C(28)-H(28)	0.95	O(15)-H(15E)	0.838(10)
C(5)-H(5B)	0.99	C(16)-N(10)	1.454(3)	C(29)-C(25)#2	1.416(4)	O(16)-H(16D)	1.0182
C(6)-N(5)	1.446(3)	C(16)-H(16)	1	C(29)-C(30)	1.476(4)	O(16)-H(16E)	0.8475
C(6)-N(2)	1.453(3)	C(17)-O(6)	1.217(3)	C(30)-O(9)	1.222(3)	O(17)-H(17D)	0.849(10)
C(6)-H(6A)	0.99	C(17)-N(12)	1.367(3)	C(30)-N(18)	1.390(3)	O(17)-H(17E)	0.849(10)
C(6)-H(6B)	0.99	C(17)-N(11)	1.383(3)	C(31)-O(10)	1.213(3)	O(18)-H(18D)	0.851(10)
C(7)-N(4)	1.450(3)	C(18)-N(13)	1.440(3)	C(31)-N(18)	1.407(3)	O(18)-H(18E)	0.853(10)
C(7)-N(7)	1.450(3)	C(18)-N(10)	1.446(3)	C(31)-C(26)#2	1.484(4)	O(1)-C(1)-N(1)	125.8(2)
C(7)-H(7A)	0.99	C(18)-H(18A)	0.99	C(32)-N(18)	1.474(3)	O(1)-C(1)-N(2)	126.1(2)
C(7)-H(7B)	0.99	C(18)-H(18B)	0.99	C(32)-C(33)	1.526(4)	N(1)-C(1)-N(2)	108.1(2)
C(8)-O(3)	1.220(3)	C(19)-N(12)	1.446(3)	C(32)-H(32A)	0.99	N(1)-C(2)-N(3)	113.9(2)
C(8)-N(5)	1.377(3)	C(19)-N(15)	1.460(3)	C(32)-H(32B)	0.99	N(1)-C(2)-C(3)	103.89(19)
C(8)-N(6)	1.377(3)	C(19)-H(19A)	0.99	C(33)-N(17)	1.512(3)	N(3)-C(2)-C(3)	103.72(19)
C(9)-N(5)	1.450(3)	C(19)-H(19B)	0.99	C(33)-H(33A)	0.99	N(1)-C(2)-H(2)	111.6
C(9)-N(7)	1.457(3)	C(20)-O(7)	1.221(3)	C(33)-H(33B)	0.99	N(3)-C(2)-H(2)	111.6
C(9)-C(10)	1.552(3)	C(20)-N(13)	1.363(3)	C(34)-N(17)	1.494(3)	C(3)-C(2)-H(2)	111.6
C(9)-H(9)	1	C(20)-N(14)	1.384(3)	C(34)-H(34A)	0.98	N(2)-C(3)-N(4)	114.3(2)
C(10)-N(6)	1.437(3)	C(21)-N(13)	1.445(3)	C(34)-H(34B)	0.98	N(2)-C(3)-C(2)	103.58(19)
C(10)-N(8)	1.449(3)	C(21)-N(15)	1.453(3)	C(34)-H(34C)	0.98	N(4)-C(3)-C(2)	103.51(19)
C(10)-H(10)	1	C(21)-C(22)	1.557(3)	C(35)-N(17)	1.506(4)	N(2)-C(3)-H(3)	111.6
C(11)-O(4)	1.225(3)	C(21)-H(21)	1	C(35)-H(35A)	0.98	N(4)-C(3)-H(3)	111.6
C(11)-N(8)	1.369(3)	C(22)-N(16)	1.442(3)	C(35)-H(35B)	0.98	C(2)-C(3)-H(3)	111.6

O(2)-C(4)-N(4)	125.6(2)	N(8)-C(11)-N(7)	108.6(2)	N(12)-C(19)-H(19A)	108.8	C(29)-C(28)-C(27)	120.7(2)
O(2)-C(4)-N(3)	126.1(2)	N(6)-C(12)-N(9)	113.1(2)	N(15)-C(19)-H(19A)	108.8	C(29)-C(28)-H(28)	119.7
N(4)-C(4)-N(3)	108.2(2)	N(6)-C(12)-H(12A)	109	N(12)-C(19)-H(19B)	108.8	C(27)-C(28)-H(28)	119.7
N(3)-C(5)-N(14)#1	112.4(2)	N(9)-C(12)-H(12A)	109	N(15)-C(19)-H(19B)	108.8	C(28)-C(29)-C(25)#2	121.0(2)
N(3)-C(5)-H(5A)	109.1	N(6)-C(12)-H(12B)	109	H(19A)-C(19)-H(19B)	107.7	C(28)-C(29)-C(30)	118.2(2)
N(14)#1-C(5)-H(5A)	109.1	N(9)-C(12)-H(12B)	109	O(7)-C(20)-N(13)	126.7(2)	C(25)#2-C(29)-C(30)	120.7(2)
N(3)-C(5)-H(5B)	109.1	H(12A)-C(12)-H(12B)	107.8	O(7)-C(20)-N(14)	125.2(2)	O(9)-C(30)-N(18)	121.3(2)
N(14)#1-C(5)-H(5B)	109.1	N(8)-C(13)-N(11)	113.6(2)	N(13)-C(20)-N(14)	108.1(2)	O(9)-C(30)-C(29)	122.3(2)
H(5A)-C(5)-H(5B)	107.9	N(8)-C(13)-H(13A)	108.8	N(13)-C(21)-N(15)	114.8(2)	N(18)-C(30)-C(29)	116.4(2)
N(5)-C(6)-N(2)	112.8(2)	N(11)-C(13)-H(13A)	108.8	N(13)-C(21)-C(22)	102.58(19)	O(10)-C(31)-N(18)	118.5(2)
N(5)-C(6)-H(6A)	109	N(8)-C(13)-H(13B)	108.8	N(15)-C(21)-C(22)	103.36(19)	O(10)-C(31)-C(26)#2	124.2(2)
N(2)-C(6)-H(6A)	109	N(11)-C(13)-H(13B)	108.8	N(13)-C(21)-H(21)	111.8	N(18)-C(31)-C(26)#2	117.3(2)
N(5)-C(6)-H(6B)	109	H(13A)-C(13)-H(13B)	107.7	N(15)-C(21)-H(21)	111.8	N(18)-C(32)-C(33)	113.4(2)
N(2)-C(6)-H(6B)	109	O(5)-C(14)-N(9)	125.8(2)	C(22)-C(21)-H(21)	111.8	N(18)-C(32)-H(32A)	108.9
H(6A)-C(6)-H(6B)	107.8	O(5)-C(14)-N(10)	126.0(2)	N(16)-C(22)-N(14)	113.7(2)	C(33)-C(32)-H(32A)	108.9
N(4)-C(7)-N(7)	113.1(2)	N(9)-C(14)-N(10)	108.3(2)	N(16)-C(22)-C(21)	103.02(19)	N(18)-C(32)-H(32B)	108.9
N(4)-C(7)-H(7A)	109	N(9)-C(15)-N(11)	115.4(2)	N(14)-C(22)-C(21)	103.58(19)	C(33)-C(32)-H(32B)	108.9
N(7)-C(7)-H(7A)	109	N(9)-C(15)-C(16)	102.7(2)	N(16)-C(22)-H(22)	112	H(32A)-C(32)-H(32B)	107.7
N(4)-C(7)-H(7B)	109	N(11)-C(15)-C(16)	102.80(19)	N(14)-C(22)-H(22)	112	N(17)-C(33)-C(32)	115.2(2)
N(7)-C(7)-H(7B)	109	N(9)-C(15)-H(15)	111.7	C(21)-C(22)-H(22)	112	N(17)-C(33)-H(33A)	108.5
H(7A)-C(7)-H(7B)	107.8	N(11)-C(15)-H(15)	111.7	O(8)-C(23)-N(16)	125.7(2)	C(32)-C(33)-H(33A)	108.5
O(3)-C(8)-N(5)	126.2(2)	C(16)-C(15)-H(15)	111.7	O(8)-C(23)-N(15)	126.2(2)	N(17)-C(33)-H(33B)	108.5
O(3)-C(8)-N(6)	126.2(2)	N(12)-C(16)-N(10)	115.1(2)	N(16)-C(23)-N(15)	108.1(2)	C(32)-C(33)-H(33B)	108.5
N(5)-C(8)-N(6)	107.6(2)	N(12)-C(16)-C(15)	103.5(2)	N(1)#1-C(24)-N(16)	113.6(2)	H(33A)-C(33)-H(33B)	107.5
N(5)-C(9)-N(7)	114.3(2)	N(10)-C(16)-C(15)	103.42(19)	N(1)#1-C(24)-H(24A)	108.9	N(17)-C(34)-H(34A)	109.5
N(5)-C(9)-C(10)	103.4(2)	N(12)-C(16)-H(16)	111.4	N(16)-C(24)-H(24A)	108.9	N(17)-C(34)-H(34B)	109.5
N(7)-C(9)-C(10)	103.22(19)	N(10)-C(16)-H(16)	111.4	N(1)#1-C(24)-H(24B)	108.9	H(34A)-C(34)-H(34B)	109.5
N(5)-C(9)-H(9)	111.8	C(15)-C(16)-H(16)	111.4	N(16)-C(24)-H(24B)	108.9	N(17)-C(34)-H(34C)	109.5
N(7)-C(9)-H(9)	111.8	O(6)-C(17)-N(12)	126.6(2)	H(24A)-C(24)-	107.7	H(34A)-C(34)-	109.5

				H(24B)		H(34C)	
C(10)-C(9)-H(9)	111.8	O(6)-C(17)-N(11)	125.8(2)	C(25)#2-C(25)-C(29)#2	117.9(3)	H(34B)-C(34)-H(34C)	109.5
N(6)-C(10)-N(8)	114.3(2)	N(12)-C(17)-N(11)	107.7(2)	C(25)#2-C(25)-C(26)	121.3(3)	N(17)-C(35)-H(35A)	109.5
N(6)-C(10)-C(9)	103.43(19)	N(13)-C(18)-N(10)	113.8(2)	C(29)#2-C(25)-C(26)	120.8(2)	N(17)-C(35)-H(35B)	109.5
N(8)-C(10)-C(9)	103.76(19)	N(13)-C(18)-H(18A)	108.8	C(27)-C(26)-C(25)	118.5(2)	H(35A)-C(35)-H(35B)	109.5
N(6)-C(10)-H(10)	111.6	N(10)-C(18)-H(18A)	108.8	C(27)-C(26)-C(31)#2	122.6(2)	N(17)-C(35)-H(35C)	109.5
N(8)-C(10)-H(10)	111.6	N(13)-C(18)-H(18B)	108.8	C(25)-C(26)-C(31)#2	118.9(2)	H(35A)-C(35)-H(35C)	109.5
C(9)-C(10)-H(10)	111.6	N(10)-C(18)-H(18B)	108.8	C(26)-C(27)-C(28)	120.6(2)	H(35B)-C(35)-H(35C)	109.5
O(4)-C(11)-N(8)	126.0(2)	H(18A)-C(18)-H(18B)	107.7	C(26)-C(27)-Br(1)	125.2(2)	N(17)-C(36)-H(36A)	109.5
O(4)-C(11)-N(7)	125.4(2)	N(12)-C(19)-N(15)	113.9(2)	C(28)-C(27)-Br(1)	114.23(19)	N(17)-C(36)-H(36B)	109.5

H(36A)-C(36)-H(36B)	109.5	C(17)-N(12)-C(19)	123.6(2)
N(17)-C(36)-H(36C)	109.5	C(16)-N(12)-C(19)	123.5(2)
H(36A)-C(36)-H(36C)	109.5	C(20)-N(13)-C(18)	122.3(2)
H(36B)-C(36)-H(36C)	109.5	C(20)-N(13)-C(21)	113.8(2)
C(1)-N(1)-C(2)	111.9(2)	C(18)-N(13)-C(21)	123.6(2)
C(1)-N(1)-C(24)#1	120.3(2)	C(20)-N(14)-C(5)#1	119.5(2)
C(2)-N(1)-C(24)#1	121.4(2)	C(20)-N(14)-C(22)	111.4(2)
C(1)-N(2)-C(3)	112.0(2)	C(5)#1-N(14)-C(22)	122.7(2)
C(1)-N(2)-C(6)	120.7(2)	C(23)-N(15)-C(21)	111.6(2)
C(3)-N(2)-C(6)	121.9(2)	C(23)-N(15)-C(19)	119.7(2)
C(4)-N(3)-C(5)	121.6(2)	C(21)-N(15)-C(19)	121.3(2)
C(4)-N(3)-C(2)	111.7(2)	C(23)-N(16)-C(22)	113.1(2)
C(5)-N(3)-C(2)	121.5(2)	C(23)-N(16)-C(24)	122.1(2)
C(4)-N(4)-C(3)	112.1(2)	C(22)-N(16)-C(24)	123.7(2)
C(4)-N(4)-C(7)	121.5(2)	C(34)-N(17)-C(36)	108.8(2)
C(3)-N(4)-C(7)	122.4(2)	C(34)-N(17)-C(35)	110.2(2)
C(8)-N(5)-C(6)	121.5(2)	C(36)-N(17)-C(35)	108.3(2)
C(8)-N(5)-C(9)	112.1(2)	C(34)-N(17)-C(33)	111.4(2)
C(6)-N(5)-C(9)	122.8(2)	C(36)-N(17)-C(33)	107.3(2)
C(8)-N(6)-C(12)	121.5(2)	C(35)-N(17)-C(33)	110.7(2)
C(8)-N(6)-C(10)	112.7(2)	C(30)-N(18)-C(31)	124.9(2)
C(12)-N(6)-C(10)	121.1(2)	C(30)-N(18)-C(32)	118.6(2)
C(11)-N(7)-C(7)	121.3(2)	C(31)-N(18)-C(32)	115.4(2)
C(11)-N(7)-C(9)	111.8(2)	H(11D)-O(11)-H(11E)	108(4)

C(7)-N(7)-C(9)	122.1(2)	H(12D)-O(12)-H(12E)	94(5)
C(11)-N(8)-C(13)	123.1(2)	H(13D)-O(13)-H(13E)	105(5)
C(11)-N(8)-C(10)	112.2(2)	H(14D)-O(14)-H(14E)	113(5)
C(13)-N(8)-C(10)	122.9(2)	H(15D)-O(15)-H(15E)	103(5)
C(14)-N(9)-C(15)	113.1(2)	H(16D)-O(16)-H(16E)	102.7
C(14)-N(9)-C(12)	121.3(2)	H(17D)-O(17)-H(17E)	104(5)
C(15)-N(9)-C(12)	125.6(2)	H(18D)-O(18)-H(18E)	115(5)
C(14)-N(10)-C(18)	119.4(2)		
C(14)-N(10)-C(16)	111.8(2)		
C(18)-N(10)-C(16)	121.5(2)		
C(17)-N(11)-C(15)	112.0(2)		
C(17)-N(11)-C(13)	121.6(2)		
C(15)-N(11)-C(13)	122.8(2)		
C(17)-N(12)-C(16)	112.9(2)		

Symmetry transformations used to generate equivalent atoms:
#1 -x+1,-y+1,-z+1 #2 -x+1,-y+2,-z+1

Table S11. Anisotropic displacement parameters ($Å^2 x\ 10^3$) for CB[8]•[2Br-NDI]. The anisotropic displacement factor exponent takes the form: $-2\pi^2[\ h^2a^{*2}U^{11} + ...\ + 2hka^*b^*U^{12}]$

	U11	U22	U33	U23	U13	U12
Br(1)	29(1)	36(1)	18(1)	-2(1)	8(1)	-6(1)
C(1)	17(1)	9(1)	17(1)	-1(1)	3(1)	0(1)
C(2)	14(1)	10(1)	16(1)	1(1)	2(1)	0(1)
C(3)	14(1)	11(1)	15(1)	-3(1)	2(1)	0(1)
C(4)	13(1)	14(1)	20(1)	-1(1)	4(1)	0(1)
C(5)	14(1)	16(1)	17(1)	2(1)	3(1)	4(1)
C(6)	26(1)	10(1)	15(1)	-1(1)	1(1)	3(1)
C(7)	13(1)	19(1)	19(1)	-4(1)	3(1)	3(1)
C(8)	18(1)	13(1)	15(1)	1(1)	5(1)	-1(1)
C(9)	16(1)	12(1)	15(1)	-1(1)	5(1)	-1(1)
C(10)	15(1)	12(1)	12(1)	1(1)	5(1)	-2(1)
C(11)	14(1)	13(1)	14(1)	-1(1)	8(1)	-1(1)
C(12)	20(1)	9(1)	15(1)	2(1)	1(1)	-2(1)
C(13)	14(1)	15(1)	14(1)	-5(1)	5(1)	-1(1)
C(14)	16(1)	13(1)	10(1)	2(1)	-1(1)	1(1)
C(15)	17(1)	12(1)	12(1)	0(1)	4(1)	-1(1)
C(16)	18(1)	11(1)	10(1)	-1(1)	3(1)	-1(1)
C(17)	20(1)	12(1)	12(1)	-2(1)	8(1)	1(1)
C(18)	15(1)	16(1)	17(1)	5(1)	1(1)	-1(1)
C(19)	21(1)	10(1)	21(1)	-2(1)	11(1)	-1(1)
C(20)	13(1)	13(1)	18(1)	1(1)	1(1)	-2(1)
C(21)	16(1)	11(1)	16(1)	0(1)	2(1)	-2(1)
C(22)	14(1)	12(1)	15(1)	0(1)	4(1)	0(1)
C(23)	17(1)	10(1)	16(1)	-4(1)	3(1)	-1(1)
C(24)	21(1)	11(1)	13(1)	2(1)	6(1)	2(1)
C(25)	12(1)	14(1)	15(1)	3(1)	3(1)	4(1)
C(26)	11(1)	17(1)	16(1)	4(1)	3(1)	4(1)
C(27)	15(1)	20(1)	15(1)	2(1)	4(1)	4(1)
C(28)	15(1)	18(1)	16(1)	1(1)	0(1)	2(1)
C(29)	12(1)	15(1)	17(1)	4(1)	2(1)	3(1)
C(30)	17(1)	17(1)	17(1)	4(1)	1(1)	1(1)
C(31)	14(1)	17(1)	20(1)	3(1)	6(1)	4(1)
C(32)	14(1)	21(1)	22(1)	3(1)	3(1)	-4(1)
C(33)	21(1)	19(1)	16(1)	1(1)	7(1)	-3(1)
C(34)	32(2)	31(2)	22(1)	4(1)	15(1)	3(1)
C(35)	37(2)	24(2)	28(2)	-4(1)	-6(1)	-8(1)
C(36)	32(2)	20(1)	21(1)	4(1)	3(1)	1(1)
I(1)	23(1)	18(1)	17(1)	1(1)	3(1)	-2(1)

N(1)	15(1)	14(1)	14(1)	0(1)	4(1)	3(1)
N(2)	14(1)	15(1)	12(1)	-1(1)	2(1)	3(1)
N(3)	18(1)	12(1)	15(1)	1(1)	3(1)	4(1)
N(4)	18(1)	13(1)	17(1)	-4(1)	2(1)	4(1)
N(5)	19(1)	14(1)	15(1)	-5(1)	2(1)	4(1)
N(6)	13(1)	13(1)	15(1)	-1(1)	2(1)	0(1)
N(7)	17(1)	11(1)	18(1)	-2(1)	0(1)	1(1)
N(8)	18(1)	10(1)	14(1)	-2(1)	3(1)	1(1)
N(9)	16(1)	9(1)	18(1)	-1(1)	4(1)	-1(1)
N(10)	14(1)	11(1)	15(1)	0(1)	4(1)	-1(1)
N(11)	15(1)	12(1)	18(1)	1(1)	3(1)	-1(1)
N(12)	17(1)	10(1)	21(1)	1(1)	5(1)	0(1)
N(13)	18(1)	11(1)	17(1)	3(1)	5(1)	1(1)
N(14)	17(1)	11(1)	17(1)	2(1)	6(1)	3(1)
N(15)	15(1)	13(1)	15(1)	1(1)	6(1)	1(1)
N(16)	16(1)	15(1)	15(1)	4(1)	4(1)	3(1)
N(17)	23(1)	18(1)	16(1)	1(1)	4(1)	-4(1)
N(18)	14(1)	16(1)	18(1)	5(1)	4(1)	-1(1)
O(1)	17(1)	23(1)	21(1)	0(1)	2(1)	8(1)
O(2)	31(1)	14(1)	26(1)	0(1)	4(1)	8(1)
O(3)	19(1)	23(1)	22(1)	-4(1)	5(1)	5(1)
O(4)	23(1)	14(1)	20(1)	-1(1)	3(1)	4(1)
O(5)	20(1)	15(1)	22(1)	-1(1)	5(1)	4(1)
O(6)	20(1)	13(1)	25(1)	0(1)	5(1)	5(1)
O(7)	24(1)	12(1)	27(1)	2(1)	7(1)	2(1)
O(8)	16(1)	21(1)	23(1)	2(1)	3(1)	2(1)
O(9)	31(1)	27(1)	17(1)	4(1)	-3(1)	-11(1)
O(10)	23(1)	22(1)	23(1)	0(1)	13(1)	-1(1)
O(11)	39(1)	22(1)	46(1)	5(1)	17(1)	0(1)
O(12)	45(2)	26(1)	67(2)	11(1)	18(1)	1(1)
O(13)	33(1)	24(1)	66(2)	10(1)	0(1)	5(1)
O(14)	46(2)	17(1)	60(2)	-6(1)	4(1)	3(1)
O(15)	45(2)	20(1)	67(2)	0(1)	29(1)	7(1)
O(16)	47(2)	70(2)	33(1)	-2(1)	7(1)	-5(1)
O(17)	39(2)	60(2)	50(2)	3(1)	-7(1)	-7(1)
O(18)	40(1)	33(1)	50(2)	1(1)	15(1)	-8(1)

Table S12. Hydrogen coordinates (x 10^4) and isotropic displacement parameters ($Å^2$x 10^3) for CB[8]•[2Br-NDI].

	x	y	z	U(eq)
H(2)	8627	7786	5595	16
H(3)	8550	7698	4459	16
H(5A)	9233	6828	6466	19
H(5B)	9059	5887	6344	19
H(6A)	6280	8153	3711	20
H(6B)	7358	8166	3583	20
H(7A)	8957	5697	3996	20
H(7B)	9052	6606	3756	20
H(9)	7911	7120	2848	16
H(10)	7126	6486	1938	16
H(12A)	5552	6515	1401	18
H(12B)	4753	6841	1818	18
H(13A)	7346	4386	2108	17
H(13B)	7041	5057	1558	17
H(15)	5356	5014	1042	16
H(16)	4094	4169	1044	16
H(18A)	2341	5010	1796	19
H(18B)	2558	4262	1342	19
H(19A)	4802	2463	2098	20
H(19B)	3958	2719	1545	20
H(21)	2443	2837	1899	17
H(22)	1746	2445	2814	16
H(24A)	2440	1545	3767	18
H(24B)	3547	1601	3990	18
H(28)	4287	8847	3614	20
H(32A)	2534	7561	5137	23
H(32B)	2283	8101	5745	23
H(33A)	3769	7471	6337	22
H(33B)	2779	7030	6324	22
H(34A)	4839	7053	5530	41
H(34B)	4053	7001	4897	41
H(34C)	4660	6223	5135	41
H(35A)	2560	6323	4978	46
H(35B)	2411	5844	5643	46
H(35C)	3134	5512	5166	46
H(36A)	4333	5466	6102	36
H(36B)	3658	5839	6595	36
H(36C)	4645	6257	6522	36

H(11D)	10210(14)	1060(20)	4990(20)	52
H(11E)	9280(20)	889(19)	4920(20)	52
H(12D)	9640(40)	2425(15)	4830(20)	68
H(12E)	9490(40)	3130(30)	4982(16)	68
H(13D)	8760(20)	3730(30)	5890(20)	62
H(13E)	9160(30)	4328(9)	5590(20)	62
H(14D)	8030(30)	3930(20)	6808(19)	62
H(14E)	7310(11)	3560(30)	6380(20)	62
H(15D)	9040(30)	3100(30)	3733(11)	64
H(15E)	8590(30)	3551(12)	3260(20)	64
H(16D)	6040	4020	6814	75
H(16E)	5364	4024	6211	75
H(17D)	3790(40)	4800(20)	4040(20)	76
H(17E)	3140(20)	4240(30)	4080(20)	76
H(18D)	3680(20)	3780(20)	5790(20)	60
H(18E)	3990(30)	4220(30)	5242(8)	60

Table S13. Torsion angles [°] for CB[8]•[2Br-NDI].

N(1)-C(2)-C(3)-N(2)	-0.8(2)	C(3)-C(2)-N(1)-C(1)	-3.8(3)	N(2)-C(6)-N(5)-C(9)	-80.7(3)
N(3)-C(2)-C(3)-N(2)	118.5(2)	N(3)-C(2)-N(1)-C(24)#1	92.3(3)	N(7)-C(9)-N(5)-C(8)	-115.5(2)
N(1)-C(2)-C(3)-N(4)	-120.3(2)	C(3)-C(2)-N(1)-C(24)#1	-155.6(2)	C(10)-C(9)-N(5)-C(8)	-4.0(3)
N(3)-C(2)-C(3)-N(4)	-1.0(2)	O(1)-C(1)-N(2)-C(3)	173.6(2)	N(7)-C(9)-N(5)-C(6)	85.6(3)
N(5)-C(9)-C(10)-N(6)	-1.4(2)	N(1)-C(1)-N(2)-C(3)	-7.7(3)	C(10)-C(9)-N(5)-C(6)	-162.9(2)
N(7)-C(9)-C(10)-N(6)	118.0(2)	O(1)-C(1)-N(2)-C(6)	18.9(4)	O(3)-C(8)-N(6)-C(12)	16.5(4)
N(5)-C(9)-C(10)-N(8)	-121.0(2)	N(1)-C(1)-N(2)-C(6)	-162.3(2)	N(5)-C(8)-N(6)-C(12)	-165.2(2)
N(7)-C(9)-C(10)-N(8)	-1.6(2)	N(4)-C(3)-N(2)-C(1)	117.0(2)	O(3)-C(8)-N(6)-C(10)	172.5(2)
N(9)-C(15)-C(16)-N(12)	-128.5(2)	C(2)-C(3)-N(2)-C(1)	5.1(3)	N(5)-C(8)-N(6)-C(10)	-9.3(3)
N(11)-C(15)-C(16)-N(12)	-8.4(2)	N(4)-C(3)-N(2)-C(6)	-88.7(3)	N(9)-C(12)-N(6)-C(8)	-117.1(2)
N(9)-C(15)-C(16)-N(10)	-8.2(2)	C(2)-C(3)-N(2)-C(6)	159.4(2)	N(9)-C(12)-N(6)-C(10)	89.0(3)
N(11)-C(15)-C(16)-N(10)	111.9(2)	N(5)-C(6)-N(2)-C(1)	-124.8(2)	N(8)-C(10)-N(6)-C(8)	118.6(2)
N(13)-C(21)-C(22)-N(16)	-126.4(2)	N(5)-C(6)-N(2)-C(3)	83.0(3)	C(9)-C(10)-N(6)-C(8)	6.6(3)
N(15)-C(21)-C(22)-N(16)	-6.7(2)	O(2)-C(4)-N(3)-C(5)	17.9(4)	N(8)-C(10)-N(6)-C(12)	-85.3(3)
N(13)-C(21)-C(22)-N(14)	-7.7(2)	N(4)-C(4)-N(3)-C(5)	-163.8(2)	C(9)-C(10)-N(6)-C(12)	162.6(2)
N(15)-C(21)-C(22)-N(14)	111.9(2)	O(2)-C(4)-N(3)-C(2)	172.8(3)	O(4)-C(11)-N(7)-C(7)	17.3(4)
C(25)#2-C(25)-C(26)-C(27)	-1.3(4)	N(4)-C(4)-N(3)-C(2)	-8.9(3)	N(8)-C(11)-N(7)-C(7)	-163.1(2)
C(29)#2-C(25)-C(26)-C(27)	178.8(2)	N(14)#1-C(5)-N(3)-C(4)	-128.9(2)	O(4)-C(11)-N(7)-C(9)	173.2(2)
C(25)#2-C(25)-C(26)-C(31)#2	178.9(3)	N(14)#1-C(5)-N(3)-C(2)	78.6(3)	N(8)-C(11)-N(7)-C(9)	-7.2(3)
C(29)#2-C(25)-C(26)-C(31)#2	-1.0(4)	N(1)-C(2)-N(3)-C(4)	118.2(2)	N(4)-C(7)-N(7)-C(11)	-124.2(2)
C(25)-C(26)-C(27)-C(28)	1.2(4)	C(3)-C(2)-N(3)-C(4)	6.0(3)	N(4)-C(7)-N(7)-C(9)	82.4(3)
C(31)#2-C(26)-C(27)-C(28)	-179.0(2)	N(1)-C(2)-N(3)-C(5)	-86.8(3)	N(5)-C(9)-N(7)-C(11)	116.9(2)
C(25)-C(26)-C(27)-Br(1)	-177.20(18)	C(3)-C(2)-N(3)-C(5)	161.0(2)	C(10)-C(9)-N(7)-C(11)	5.4(3)
C(31)#2-C(26)-C(27)-Br(1)	2.6(4)	O(2)-C(4)-N(4)-C(3)	-173.5(3)	N(5)-C(9)-N(7)-C(7)	-87.4(3)
C(26)-C(27)-C(28)-C(29)	0.1(4)	N(3)-C(4)-N(4)-C(3)	8.1(3)	C(10)-C(9)-N(7)-C(7)	161.0(2)
Br(1)-C(27)-C(28)-C(29)	178.65(19)	O(2)-C(4)-N(4)-C(7)	-15.6(4)	O(4)-C(11)-N(8)-C(13)	-9.2(4)
C(27)-C(28)-C(29)-C(25)#2	-1.3(4)	N(3)-C(4)-N(4)-C(7)	166.1(2)	N(7)-C(11)-N(8)-C(13)	171.2(2)
C(27)-C(28)-C(29)-C(30)	-178.6(2)	N(2)-C(3)-N(4)-C(4)	-116.1(2)	O(4)-C(11)-N(8)-C(10)	-174.4(2)
C(28)-C(29)-C(30)-O(9)	-6.7(4)	C(2)-C(3)-N(4)-C(4)	-4.2(3)	N(7)-C(11)-N(8)-C(10)	6.0(3)
C(25)#2-C(29)-C(30)-O(9)	175.9(2)	N(2)-C(3)-N(4)-C(7)	86.1(3)	N(11)-C(13)-N(8)-C(11)	112.3(3)
C(28)-C(29)-C(30)-N(18)	173.2(2)	C(2)-C(3)-N(4)-C(7)	-162.0(2)	N(11)-C(13)-N(8)-C(10)	-84.2(3)
C(25)#2-C(29)-C(30)-N(18)	-4.1(4)	N(7)-C(7)-N(4)-C(4)	123.7(3)	N(6)-C(10)-N(8)-C(11)	-114.5(2)
N(18)-C(32)-C(33)-N(17)	-90.8(3)	N(7)-C(7)-N(4)-C(3)	-80.6(3)	C(9)-C(10)-N(8)-C(11)	-2.6(3)
O(1)-C(1)-N(1)-C(2)	-174.2(2)	O(3)-C(8)-N(5)-C(6)	-14.4(4)	N(6)-C(10)-N(8)-C(13)	80.4(3)
N(2)-C(1)-N(1)-C(2)	7.1(3)	N(6)-C(8)-N(5)-C(6)	167.4(2)	C(9)-C(10)-N(8)-C(13)	-167.7(2)
O(1)-C(1)-N(1)-C(24)#1	-22.0(4)	O(3)-C(8)-N(5)-C(9)	-173.6(2)	O(5)-C(14)-N(9)-C(15)	178.9(2)
N(2)-C(1)-N(1)-C(24)#1	159.3(2)	N(6)-C(8)-N(5)-C(9)	8.2(3)	N(10)-C(14)-N(9)-C(15)	-2.4(3)
N(3)-C(2)-N(1)-C(1)	-115.9(2)	N(2)-C(6)-N(5)-C(8)	122.4(3)	O(5)-C(14)-N(9)-C(12)	-1.1(4)

N(10)-C(14)-N(9)-C(12)	177.6(2)	N(14)-C(20)-N(13)-C(18)	-176.2(2)	C(32)-C(33)-N(17)-C(36)	176.3(2)
N(11)-C(15)-N(9)-C(14)	-104.2(2)	O(7)-C(20)-N(13)-C(21)	178.6(2)	C(32)-C(33)-N(17)-C(35)	-65.7(3)
C(16)-C(15)-N(9)-C(14)	6.8(3)	N(14)-C(20)-N(13)-C(21)	-2.2(3)	O(9)-C(30)-N(18)-C(31)	-169.1(2)
N(11)-C(15)-N(9)-C(12)	75.8(3)	N(10)-C(18)-N(13)-C(20)	99.7(3)	C(29)-C(30)-N(18)-C(31)	11.0(4)
C(16)-C(15)-N(9)-C(12)	-173.2(2)	N(10)-C(18)-N(13)-C(21)	-73.6(3)	O(9)-C(30)-N(18)-C(32)	-1.0(4)
N(6)-C(12)-N(9)-C(14)	96.9(3)	N(15)-C(21)-N(13)-C(20)	-104.9(2)	C(29)-C(30)-N(18)-C(32)	179.0(2)
N(6)-C(12)-N(9)-C(15)	-83.0(3)	C(22)-C(21)-N(13)-C(20)	6.4(3)	O(10)-C(31)-N(18)-C(30)	169.0(2)
O(5)-C(14)-N(10)-C(18)	24.5(4)	N(15)-C(21)-N(13)-C(18)	68.9(3)	C(26)#2-C(31)-N(18)-C(30)	-11.5(4)
N(9)-C(14)-N(10)-C(18)	-154.2(2)	C(22)-C(21)-N(13)-C(18)	-179.7(2)	O(10)-C(31)-N(18)-C(32)	0.5(3)
O(5)-C(14)-N(10)-C(16)	175.1(2)	O(7)-C(20)-N(14)-C(5)#1	23.0(4)	C(26)#2-C(31)-N(18)-C(32)	-179.9(2)
N(9)-C(14)-N(10)-C(16)	-3.6(3)	N(13)-C(20)-N(14)-C(5)#1	-156.2(2)	C(33)-C(32)-N(18)-C(30)	119.1(3)
N(13)-C(18)-N(10)-C(14)	-116.4(2)	O(7)-C(20)-N(14)-C(22)	175.7(2)	C(33)-C(32)-N(18)-C(31)	-71.7(3)
N(13)-C(18)-N(10)-C(16)	95.9(3)	N(13)-C(20)-N(14)-C(22)	-3.4(3)		
N(12)-C(16)-N(10)-C(14)	119.6(2)	N(16)-C(22)-N(14)-C(20)	118.2(2)		
C(15)-C(16)-N(10)-C(14)	7.5(3)	C(21)-C(22)-N(14)-C(20)	7.1(3)		
N(12)-C(16)-N(10)-C(18)	-90.5(3)	N(16)-C(22)-N(14)-C(5)#1	-90.1(3)		
C(15)-C(16)-N(10)-C(18)	157.4(2)	C(21)-C(22)-N(14)-C(5)#1	158.8(2)		
O(6)-C(17)-N(11)-C(15)	169.4(2)	O(8)-C(23)-N(15)-C(21)	172.1(2)		
N(12)-C(17)-N(11)-C(15)	-9.6(3)	N(16)-C(23)-N(15)-C(21)	-8.1(3)		
O(6)-C(17)-N(11)-C(13)	10.3(4)	O(8)-C(23)-N(15)-C(19)	21.8(4)		
N(12)-C(17)-N(11)-C(13)	-168.6(2)	N(16)-C(23)-N(15)-C(19)	-158.4(2)		
N(9)-C(15)-N(11)-C(17)	122.2(2)	N(13)-C(21)-N(15)-C(23)	120.1(2)		
C(16)-C(15)-N(11)-C(17)	11.2(3)	C(22)-C(21)-N(15)-C(23)	9.2(3)		
N(9)-C(15)-N(11)-C(13)	-79.1(3)	N(13)-C(21)-N(15)-C(19)	-90.2(3)		
C(16)-C(15)-N(11)-C(13)	170.0(2)	C(22)-C(21)-N(15)-C(19)	159.0(2)		
N(8)-C(13)-N(11)-C(17)	-116.6(3)	N(12)-C(19)-N(15)-C(23)	-117.3(3)		
N(8)-C(13)-N(11)-C(15)	86.6(3)	N(12)-C(19)-N(15)-C(21)	95.4(3)		
O(6)-C(17)-N(12)-C(16)	-175.6(2)	O(8)-C(23)-N(16)-C(22)	-176.9(2)		
N(11)-C(17)-N(12)-C(16)	3.4(3)	N(15)-C(23)-N(16)-C(22)	3.2(3)		
O(6)-C(17)-N(12)-C(19)	7.4(4)	O(8)-C(23)-N(16)-C(24)	-8.4(4)		
N(11)-C(17)-N(12)-C(19)	-173.7(2)	N(15)-C(23)-N(16)-C(24)	171.8(2)		
N(10)-C(16)-N(12)-C(17)	-108.6(2)	N(14)-C(22)-N(16)-C(23)	-108.9(2)		
C(15)-C(16)-N(12)-C(17)	3.4(3)	C(21)-C(22)-N(16)-C(23)	2.4(3)		
N(10)-C(16)-N(12)-C(19)	68.4(3)	N(14)-C(22)-N(16)-C(24)	82.7(3)		
C(15)-C(16)-N(12)-C(19)	-179.5(2)	C(21)-C(22)-N(16)-C(24)	-165.9(2)		
N(15)-C(19)-N(12)-C(17)	103.7(3)	N(1)#1-C(24)-N(16)-C(23)	115.8(3)		
N(15)-C(19)-N(12)-C(16)	-73.0(3)	N(1)#1-C(24)-N(16)-C(22)	-76.9(3)		
O(7)-C(20)-N(13)-C(18)	4.7(4)	C(32)-C(33)-N(17)-C(34)	57.3(3)		

Symmetry transformations used to generate equivalent atoms:
#1 -x+1,-y+1,-z+1 #2 -x+1,-y+2,-z+1

Time-dependent density functional theory (TDDFT) simulation

Table S14. Singlet and triplet excited states energy levels and transition orbital contribution for 2Br-NDI.

Excited state level	Singlet		Triplet	
	Energy/eV	Transition orbital contribution	Energy/eV	Transition orbital contribution
1	2.7530	H-1→L 91.3% H→L 5.7%	2.0010	H → L 81.1%, H-3 → L 13.9%
2	2.7610	H-2 → L 96.7%	2.4670	H-3 → L 79.1% H → L 15.6%
3	2.8510	H → L 91.0% H-1→ L 5.6%	2.6190	H-2 → L 92.5%
4	3.5080	H-3 →L 92.8%	2.6210	H-1 → L 92.9%
5	3.5540	H-5 → L 90.2% H-4 → L 5.0%	3.0780	H-4 → L 80.7% H → L+1 13.2%
6	3.5710	H-4 → L 93.3%	3.3340	H-5 → L 87.9%
7	3.7730	H-6→ L 79.5% H-7 → L 13.6%	3.4220	H-8 → L 21.7% H-11 → L 20.8% H → L+1 20.0% H-3 → L+1 19.1% H-4 → L 9.8%
8	4.1040	H → L+1 81.4% H-8 → L 16.9%	3.5100	H-6 → L 84.3%
9	4.1350	H-9 → L 90.5%	3.6170	H-7 → L 85.8%
10	4.1930	H-7 → L 75.6% H-6 → L 11.1% H-10 → L 6.2%	3.7490	H-8 → L 68.6% H-11 → L 9.9% H-3 → L+1 7.7% H → L+1 5.4%

Table S15. Singlet and triplet excited states energy levels and transition orbital contribution for CB[8]·(2Br-NDI).

Excited state level	Singlet		Triplet	
	Energy/eV	Transition orbital contribution	Energy/eV	Transition orbital contribution
1	2.6120	H → L 98.1%	2.0480	H-18 → L 65.3% H-49 → L 15.7%
2	2.6130	H-1 → L 98.2%	2.5810	H-49 → L 49.6% H-18 → L 22.3% H-48 → L 5.0%
3	2.8000	H-2 → L 97.6%	2.6120	H → L 97.6%
4	2.8010	H-3 → L 97.6%	2.6120	H-1 → L 97.7%
5	2.8760	H-4 → L 91.6%	2.7760	H-41 → L 47.9% H-39 → L 13.4% H-42 → L 7.4% H-44 → L 5.0%
6	2.8780	H-5 → L 92.0%	2.7920	H-42 → L 35.5% H-2 → L 17.6% H-3 → L 16.6% H-40 → L 6.7% H-41 → L 5.0%
7	2.9480	H-41 → L 44.4% H-39 → L 13.5% H-7 → L 9.2% H-42 → L 6.9%	2.8020	H-2 → L 57.4% H-3 → L 33.1%
8	2.9580	H-42 → L 37.1% H-6 → L 20.7% H-40 → L 7.7% H-41 → L 5.3%	2.8060	H-3 → L 45.2% H-2 → L 19.3% H-42 → L 17.7%

9	2.9780	H-7 → L 64.0% H-6 → L 10.5% H-41 → L 7.5%	2.8780	H-4 → L	87.8%
10	2.9810	H-6 → L 53.1% H-42 → L 18.8% H-7 → L 7.3%	2.8790	H-5 → L	88.0%

Table S16. Spin-orbit coupling matrix element (SOCME, $<^1\Psi|\hat{H}_{SOC}|^3\Psi>$) between S_n and T_n.

S	T	2Br-NDI $<^1\Psi\|\hat{H}_{SOC}\|^3\Psi>$ cm^{-1}	CB[8]·(2Br-NDI) $<^1\Psi\|\hat{H}_{SOC}\|^3\Psi>$ cm^{-1}
1	1	485.6274781	3.975198108
1	2	400.7881307	6.716911493
1	3	17.9868035	0.191049732
1	4	153.0561678	0.175783958
1	5	20.4601002	3.771326027
1	6	1.108241851	4.42648845
1	7	4.403385062	6.855289928
1	8	123.0833758	3.876712525
1	9	71.56189838	4.918831162
1	10	6.260487201	1.045466403
2	1	13.23514639	4.038044081
2	2	8.976263142	6.862477687
2	3	8.82077661	0.166132477
2	4	2.801517446	0.202484567
2	5	723.2485499	3.240277766
2	6	34.31680201	4.784025502
2	7	199.4841781	4.821732054
2	8	1.872965563	6.228876303
2	9	0.629285309	1.136133795
2	10	238.898825	4.957600226
3	1	115.952282	8.805838972
3	2	91.22524925	14.88948958
3	3	73.09210765	8.593584817
3	4	618.5612634	0.761248974
3	5	0.886397202	1.861424186
3	6	0.950157882	4.516525213
3	7	0.41484937	1.23032516
3	8	208.0245123	3.069429914
3	9	215.5920768	5.512939325
3	10	0.779807669	1.555827754
4	1	36.47522173	8.55680431
4	2	30.12791729	14.55979739

4	3	2.061504305	1.008811182
4	4	112.6332726	8.584509305
4	5	1.729797676	1.398749441
4	6	6.130081566	4.58293574
4	7	0.540925133	0.130384048
4	8	46.51936156	3.266037354
4	9	51.28035296	1.216100325
4	10	2.614364167	5.541768671
5	1	1.050142847	17.63796474
5	2	0.262488095	29.63753532
5	3	153.7347043	5.319454859
5	4	19.0416097	0.956504051
5	5	287.2622391	3.999537473
5	6	65.69369757	4.873284313
5	7	78.17247661	7.380650378
5	8	0.197230829	7.217076971
5	9	0.914986339	1.574134683
5	10	77.53803841	0.339705755
6	1	0.384447656	18.32193767
6	2	0.602162769	31.0094018
6	3	700.5960186	0.951367437
6	4	83.51452389	5.395905855
6	5	67.59163336	2.941530214
6	6	304.258859	5.519257196
6	7	27.24073604	3.526839945
6	8	1.434782213	9.846263251
6	9	0.259807621	0.871206061
6	10	108.3394577	1.244909635
7	1	218.0547956	12.87591938
7	2	199.9313995	20.5166274
7	3	6.362240172	3.906520191
7	4	53.59961194	3.920522924
7	5	2.075716744	6.341561322
7	6	0.091104336	0.611064645
7	7	0.243515913	2.392488244
7	8	28.96083735	0.327871926
7	9	52.6535317	10.78862827
7	10	0.376297754	6.726849188
8	1	0.03	198.6057978
8	2	0.041231056	334.3689026

8	3	10.23508183	6.05264405
8	4	0.968194195	5.848221952
8	5	13.96788817	0.663927707
8	6	13.44697364	6.967165851
8	7	7.492789868	0.404227659
8	8	0.146969385	1.555442059
8	9	0.177482393	2.057692883
8	10	7.523243981	2.498659641
9	1	1.726731016	15.81580855
9	2	0.374966665	26.22427311
9	3	96.80194936	3.593897606
9	4	11.41780189	3.137674298
9	5	445.233815	8.798920388
9	6	47.49413122	2.813982942
9	7	191.2510625	6.22552809
9	8	1.183004649	2.101618424
9	9	1.035615759	5.758376507
9	10	149.811549	2.858723491
10	1	105.0252984	135.1359012
10	2	97.65505517	228.0191036
10	3	17.60699009	2.431234254
10	4	159.3438188	2.278354669
10	5	1.688608895	0.867870958
10	6	0.511272921	27.32566742
10	7	1.305565012	4.402328929
10	8	78.38739376	22.94832674
10	9	15.50782061	5.740435524
10	10	0.41484937	9.894215482

Table S17. Energy gap between S_n and T_n for 2Br-NDI.

ΔE_{ST}	S_1	S_2	S_3	S_4	S_5	S_6	S_7	S_8	S_9	S_{10}
T1	0.752	0.76	0.85	1.507	1.553	1.57	1.772	2.103	2.134	2.192
T2	0.286	0.294	0.384	1.041	1.087	1.104	1.306	1.637	1.668	1.726
T3	0.134	0.142	0.232	0.889	0.935	0.952	1.154	1.485	1.516	1.574
T4	0.132	0.14	0.23	0.887	0.933	0.95	1.152	1.483	1.514	1.572
T5	-0.325	-0.317	-0.227	0.43	0.476	0.493	0.695	1.026	1.057	1.115
T6	-0.581	-0.573	-0.483	0.174	0.22	0.237	0.439	0.77	0.801	0.859
T7	-0.669	-0.661	-0.571	0.086	0.132	0.149	0.351	0.682	0.713	0.771
T8	-0.757	-0.749	-0.659	-0.002	0.044	0.061	0.263	0.594	0.625	0.683
T9	-0.864	-0.856	-0.766	-0.109	-0.063	-0.046	0.156	0.487	0.518	0.576

T10	-0.996	-0.988	-0.898	-0.241	-0.195	-0.178	0.024	0.355	0.386	0.444

Table S18. Energy gap between S_n and T_n for the CB[8]·(2Br-NDI) complex.

ΔE_{ST}	S1	S2	S3	S4	S5	S6	S7	S8	S9	S10
T1	0.564	0.565	0.752	0.753	0.828	0.83	0.9	0.91	0.93	0.933
T2	0.031	0.032	0.219	0.22	0.295	0.297	0.367	0.377	0.397	0.4
T3	0	0.001	0.188	0.189	0.264	0.266	0.336	0.346	0.366	0.369
T4	0	0.001	0.188	0.189	0.264	0.266	0.336	0.346	0.366	0.369
T5	-0.164	-0.163	0.024	0.025	0.1	0.102	0.172	0.182	0.202	0.205
T6	-0.18	-0.179	0.008	0.009	0.084	0.086	0.156	0.166	0.186	0.189
T7	-0.19	-0.189	-0.002	-0.001	0.074	0.076	0.146	0.156	0.176	0.179
T8	-0.194	-0.193	-0.006	-0.005	0.07	0.072	0.142	0.152	0.172	0.175
T9	-0.266	-0.265	-0.078	-0.077	-0.002	0	0.07	0.08	0.1	0.103
T10	-0.267	-0.266	-0.079	-0.078	-0.003	-0.001	0.069	0.079	0.099	0.102

Table S 19. Change (Δ) of $|\langle^1\Psi|\hat{H}_{SOC}|^3\Psi\rangle|^2/\exp(\Delta E^2_{ST})$ of 2Br-NDI upon addition of CB[8].

S	T	$\lvert\langle^1\Psi\rvert\hat{H}_{SOC}\rvert^3\Psi\rangle\rvert^2/\exp(\Delta E^2_{ST})$		Δ
		2Br-NDI	CB[8]•(2Br-NDI)	
1	1	133971.1354	11.49662105	-133959.6388
1	2	148015.1438	45.07356349	-147970.0702
1	3	317.7677277	0.0365	-317.7312277
1	4	23021.54804	0.0309	-23021.51714
1	5	376.6544976	13.84545945	-362.8090382
1	6	0.876331078	18.9691351	18.09280402
1	7	12.39367367	45.32873749	32.93506382
1	8	8541.35514	14.47378402	-8526.881356
1	9	2427.530037	22.54212694	-2404.98791
1	10	14.53413498	1.017793663	-13.51634132
2	1	98.31256019	11.84962087	-86.46293933
2	2	73.90136725	47.04540084	-26.85596641
2	3	76.25292949	0.027599972	-76.22532952
2	4	7.696167139	0.040999959	-7.65516718
2	5	473078.6241	10.22411466	-473068.3999
2	6	848.0513408	22.1652045	-825.8861363
2	7	25707.77747	22.43327666	-25685.3442
2	8	2.001796594	37.38026516	35.37846857
2	9	0.190314547	1.203263178	1.012948632
2	10	21502.75342	22.89887074	-21479.85455
3	1	6528.010393	44.05003038	-6483.960363
3	2	7181.096951	211.315047	-6969.781904
3	3	5062.505454	71.285144	-4991.22031

3	4	362903.5869	0.55937588	-362903.0275
3	5	0.746239087	3.462904792	2.716665706
3	6	0.714949596	20.39769451	19.68274491
3	7	0.12421758	1.513693945	1.389476365
3	8	28030.0055	9.421060836	-28020.58444
3	9	25848.81863	30.20815338	-25818.61048
3	10	0.271492725	2.405540079	2.134047354
4	1	137.3067325	41.53118473	-95.77554777
4	2	307.1153632	201.9718344	-105.1435288
4	3	1.928130582	0.981988363	-0.946142219
4	4	5776.223255	71.10784518	-5705.115409
4	5	2.487078934	1.95527757	-0.531801364
4	6	36.45724163	21.0015988	-15.45564283
4	7	0.290443913	0.016999983	-0.27344393
4	8	2164.042344	10.66673333	-2153.37561
4	9	2598.616303	1.470157545	-2597.146146
4	10	6.449230617	30.5249203	24.07568968
5	1	0.09886929	156.7298045	156.6309352
5	2	0.021138313	805.173906	805.1527677
5	3	9859.905218	26.39159679	-9833.513621
5	4	151.8304045	0.853306472	-150.977098
5	5	65789.46823	15.83713416	-65773.63109
5	6	4111.758138	23.58191757	-4088.176221
5	7	6005.381412	54.17651563	-5951.204897
5	8	0.038824762	51.83160189	51.79277713
5	9	0.833883739	2.477890088	1.64400635
5	10	5787.827407	0.115398961	-5787.712008
6	1	0.012565563	168.5610912	168.5485257
6	2	0.107177281	880.3960691	880.2888918
6	3	198304.47	0.843271892	-198303.6267
6	4	2828.611151	27.12687631	-2801.484275
6	5	3582.869938	8.563045022	-3574.306893
6	6	87517.03141	30.23773267	-87486.79368
6	7	725.7648055	12.36696174	-713.3978437
6	8	2.050954183	96.44761735	94.39666317
6	9	0.067357321	0.759	0.691642679
6	10	11371.37884	1.54979845	-11369.82905
7	1	2058.038811	73.7527074	-1984.286103
7	2	7261.288782	367.8893819	-6893.3994
7	3	10.68718208	13.63170053	2.94451845

7	4	762.025223	13.72960003	-748.295623
7	5	2.658037385	39.04309386	36.38505647
7	6	0.00684511	0.364422617	0.357577508
7	7	0.052426296	5.603278437	5.550852141
7	8	782.6768961	0.105354078	-782.5715421
7	9	2705.739753	115.825562	-2589.914191
7	10	0.141518462	45.03557441	44.89405594
8	1	1.08026E-05	17232.35307	17232.35306
8	2	0.000116584	96989.7677	96989.76758
8	3	11.54690491	32.50111575	20.95421084
8	4	0.103940756	30.34280283	30.23886208
8	5	68.09106403	0.426438115	-67.66462591
8	6	99.94381166	47.22205461	-52.72175706
8	7	35.26032571	0.159471494	-35.10085422
8	8	0.015178156	2.36414297	2.348964813
8	9	0.024849026	4.20708829	4.182239264
8	10	49.89744758	6.204456901	-43.69299068
9	1	0.03138278	105.3322839	105.3009011
9	2	0.008703237	587.4328095	587.4241063
9	3	941.1271609	11.29678978	-929.8303711
9	4	13.17276464	8.610718049	-4.562046593
9	5	64857.64967	74.32549744	-64783.32417
9	6	1187.506845	7.649236156	-1179.857609
9	7	22000.16113	37.57506047	-21962.58607
9	8	0.946949068	4.288047289	3.341098222
9	9	0.82009784	32.82896343	32.00886559
9	10	19336.70395	8.092594522	-19328.61135
10	1	90.3362226	7647.032137	7556.695915
10	2	484.8341378	44305.26626	43820.43212
10	3	26.02651887	5.158454938	-20.86806393
10	4	2145.106543	4.530109415	-2140.576433
10	5	0.822493336	0.722202663	-0.100290673
10	6	0.124982134	720.4902752	720.3652931
10	7	0.940664078	18.76937225	17.82870818
10	8	3853.885893	510.7422447	-3343.143648
10	9	172.5889756	32.60485375	-139.9841218
10	10	0.141307689	96.88227515	96.74096746

References

1 A. A. Berezin, A. Sciutto, N. Demitri and D. Bonifazi, *Org. Lett.*, 2015, **17**, 1870-1873.
2 R. Fernando, F. Etheridge, E. Muller and G. Sauvé, *New J. Chem.*, 2015, **39**, 2506-2514.
3 M. Nadai, F. Doria, M. Di Antonio, G. Sattin, L. Germani, C. Percivalle, M. Palumbo, S. N. Richter and M. Freccero, *Biochimie*, 2011, **93**, 1328-1340.
4 F. Doria, M. Nadai, G. Sattin, L. Pasotti, S. N. Richter and M. Freccero, *Org. Biomol. Chem.*, 2012, **10**, 3830-3840.
5 S. Kuila, K. V. Rao, S. Garain, P. K. Samanta, S. Das, S. K. Pati, M. Eswaramoorthy and S. J. George, *Angew. Chem., Int. Ed.*, 2018, **57**, 17115-17119.
6 X. R. Yang, Z. Y. Zhao, X. Z. Zhang and S. M. Liu, *Sci. China. Chem.*, 2018, **61**, 787-791.
7 H. Cong, X. L. Ni, X. Xiao, Y. Huang, Q.-J. Zhu, S.-F. Xue, Z. Tao, L. F. Lindoy and G. Wei, *Org. Biomol. Chem.*, 2016, **14**, 4335-4364.
8 F. B. Liu, S. Chowdhury, R. Rosas, V. Monnier, L. Charles, H. Karoui, D. Gigmes, O. Ouari, F. Chevallier, C. Bucher, A. Kermagoret, S. M. Liu and D. Bardelang, *Org. Lett.*, 2021, **23**, 5283-5287.
9 https://d31kydh6n6r5j5.cloudfront.net/uploads/sites/80/2019/06/MNova_2D_NMR_Processing_6_2015.pdf
10 https://mestrelab.com/software/freeware/
11 F. Neese, *WIREs Computational Molecular Science*, 2018, **8**, e1327.
12 J. G. Brandenburg, C. Bannwarth, A. Hansen and S. Grimme, *The Journal of Chemical Physics*, 2018, **148**, 064104.
13 A. D. Becke, *The Journal of Chemical Physics*, 1997, **107**, 8554-8560.
14 S. Grimme, S. Ehrlich and L. Goerigk, *J. Comput. Chem.*, 2011, **32**, 1456-1465.
15 T. Lu and F. Chen, *J. Comput. Chem.*, 2012, **33**, 580-592.
16 W. Humphrey, A. Dalke and K. Schulten, *J. Mol. Graphics*, 1996, **14**, 33-38.